Studies by the U.S. Geological Survey in Alaska, 2001
U.S. Geological Survey Professional Paper 1678

Trident Volcano: Four Contiguous Stratocones Adjacent to Katmai Pass, Alaska Peninsula

By Wes Hildreth, Judy Fierstein, Marvin A. Lanphere, and David F. Siems

> "It was thither the travellers were bound, headed toward Katmai Pass, which is no more than a gap between peaks, through which the hibernal gales suck and swirl. This pass is even balder than the surrounding barrens, for it forms a funnel at each end, confining the winds and affording them freer course… [Later] the storm was upon them, sweeping through the chute wherein they stood with rapidly increasing violence… It was Dante's third circle of hell let loose—Cerberus baying through his wide, threefold throat, and the voices of tormented souls shrilling through the infernal shades. It came from behind them, lifting the fur on the backs of the wolf-dogs and filling it with powder, pelting their hides with sharp particles until they refused to stand before it…"
>
> Rex Beach, *The Silver Horde* (1909)

Abstract

Trident Volcano lies between Katmai Pass and Mount Katmai along the volcanic front of the Alaska Peninsula reach of the Aleutian Arc. Trident consists of four contiguous stratovolcanoes and several peripheral lava domes, all andesitic-dacitic in composition. Construction of the four principal edifices proceeded stepwise from northeast to southwest. The oldest edifice, East Trident, grew into a 7-km^3-volume stratocone, about 1,000 m high, during a brief eruptive lifetime around 143±8 ka. The central and highest peak, Trident I, buttressed by East Trident, grew into an adjacent 8-km^3-volume stratocone and ended its activity by about 58±15 ka. The third center, West Trident, is a 900-m-high edifice that overlaps the west flank of Trident I; accumulation of its 3- to 4-km^3 eruptive volume was largely completed by 44±12 ka. After glacial dissection of the three Pleistocene cones, a fourth edifice, Southwest Trident, was constructed between 1953 and 1974, overlapping the southwest flanks of two of the older cones. The young volcano produced about 0.7 km^3 of lava and ejecta, including four blocky lava flows and a 3-km^2-area composite cone that remains fumarolically active. Several glaciated dacitic lava domes at the periphery of the Trident group have compositional affinity with the main cones, and all of the lava domes appear to predate some of the lava flows that issued from West Trident and Trident I. The only domes dated are Falling Mountain (70±8 ka) and Mount Cerberus (114±46 ka), which together frame the entrance to Katmai Pass. Two clusters of warm springs and two fields of sulfurous fumaroles have been studied by other workers. Geophysical anomalies that are centered near Katmai Pass and overlap the western part of the Trident group include traveltime delays and attenuation of seismic waves, a Bouguer gravity low, hundreds of small shallow earthquakes each year, and several centimeters of recent uplift detected by synthetic-aperture-radar interferometry. Reconstruction of the eroded edifices yields an estimated eruptive volume for the whole Trident group of 21±4 km^3. Averaged over 143±8 k.y., this output gives a long-term eruption rate of 0.11 to 0.18 km^3/k.y., far smaller than the rates calculated for neighboring Mageik and Katmai Volcanoes.

Introduction

Trident Volcano is actually a group of four stratovolcanoes and several lava domes, part of the Katmai volcanic cluster on the upper Alaska Peninsula (fig. 1). As the main summits of Trident form part of the peninsular drainage divide, their eruptive products have flowed down both sides of the volcanic axis. Eruptive activity at Trident began by 143 ka, before initiation of the neighboring Mageik and Katmai Volcanoes. Accordingly, most components of the Trident group have been sharply dissected during several periods of glacial expansion. From Trident, nonetheless, there also issued the Katmai cluster's most recent eruptive episode, which built a new stratocone and a derivative lava-flow apron between 1953 and 1974. Of the several volcanoes in the Katmai cluster (fig. 1), Trident is the closest to Novarupta (fig. 2), where a new vent opened through Jurassic basement rocks in 1912 to release the world's most voluminous 20th-century eruption (Fierstein and Hildreth,

1992). In the course of studying the products of that eruption, we undertook a detailed reconnaissance of the Trident group (fig. 3), much of which is blanketed by 1912 pumice-fall deposits (figs. 3, 4). We report the results of that reconnaissance investigation here.

Previous Work

Trident was named during the National Geographic Society expedition of 1916, which began as an investigation into the ecologic effects of the 1912 eruption (Griggs, 1922). The fine 1916 photograph of Trident (Griggs, 1922, p. 98), a view northwestward from the mouth of Mageik Creek canyon (a site just east of that of our fig. 4), actually shows the fourth peak of the group (West Trident, figs. 2–4), in addition to the three higher summits prominent from that viewpoint. Evidently, however, the name "Quadrident" lacked sufficient euphony to appeal to Griggs' late Edwardian taste. Just as well, as a fifth summit was constructed after 1953.

Trident received little attention before the onset of its eruption in 1953. After crossing Katmai Pass in 1898, Spurr (1900) noted that two volcanoes (then unnamed) flank the pass, and he mentioned thermal springs south of the pass. Reporting on his 1915–19 expeditions, Griggs repeatedly

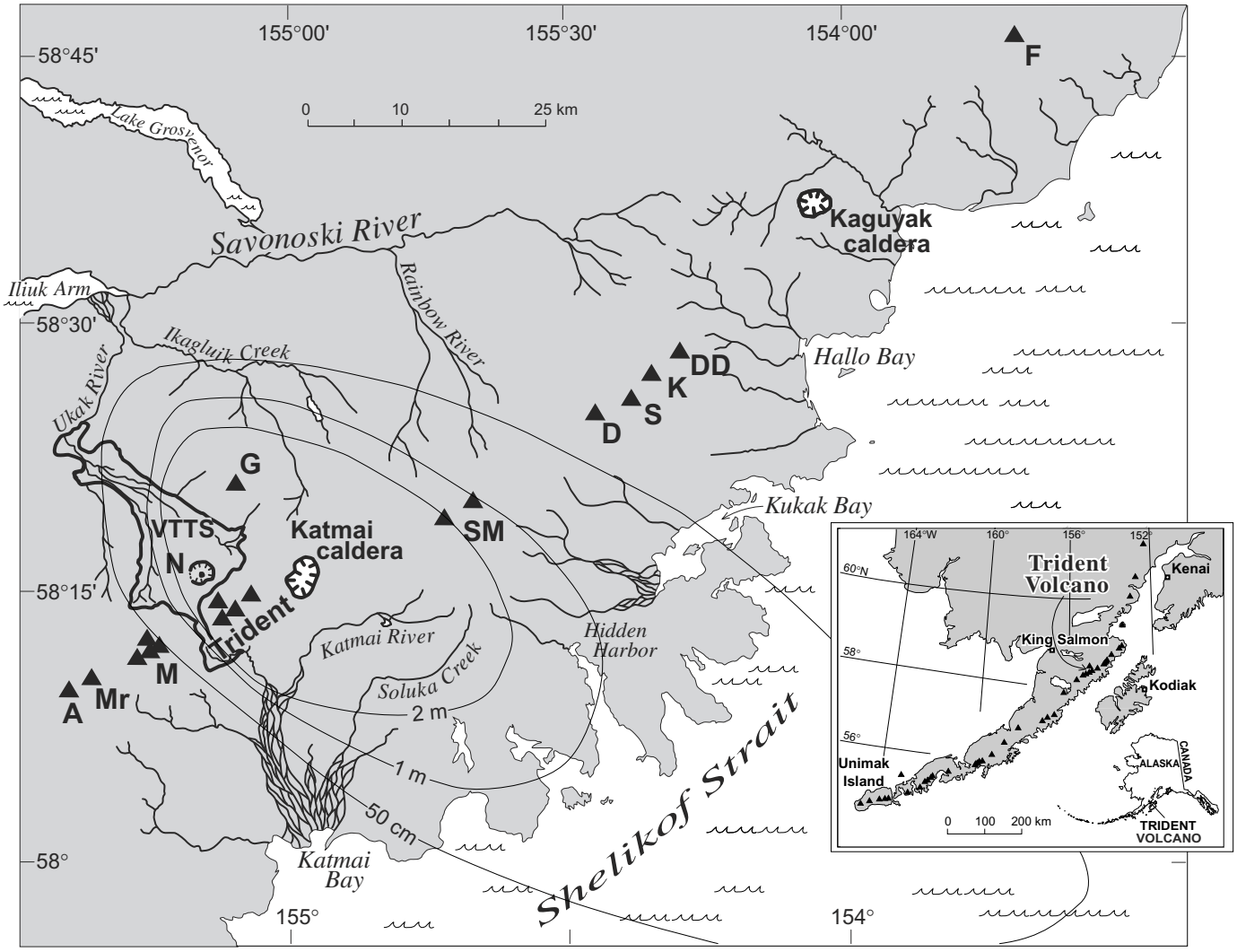

Figure 1. Southern Alaska, showing location of Trident Volcano, a cluster of four cones, along late Quaternary volcanic axis, which straddles drainage divide on this stretch of the Alaska Peninsula. Triangles, andesite-dacite stratovolcanoes: A, Alagogshak; D, Denison; DD, Devils Desk; F, Fourpeaked, G, Griggs; K, Kukak; M, Mageik (cluster of four); Mr, Martin; S, Steller; SM, Snowy Mountain (two cones). VTTS, Valley of Ten Thousand Smokes ash-flow sheet (outlined area), which erupted at Novarupta (N) in June 1912 and also poured southward through Katmai Pass between Trident and Mageik Volcanoes. Isopachs show thickness of cumulative plinian fallout from Novarupta, originally 2 to 10 m thick over Trident Volcano. Inset shows town of King Salmon just west of elongate Naknek Lake, of which the Iliuk Arm is southeastern branch.

referred to Trident as an "old volcano"; he, too, mentioned the thermal springs at its southwest toe, and he illustrated a fumarolic plume on its southeast flank (Griggs, 1922, p. 98). Sporadic observations of the 1953–74 eruptive activity were summarized by Muller and others (1954), Snyder (1954), Decker (1963), Ward and Matumoto (1967), and Simkin and Siebert (1994). The 1953–63 eruptive products were studied petrologically by Ray (1967) and in detail, analytically and experimentally, by Coombs and others (2000). Several unlocated grab samples from the prehistoric edifices of Trident were studied petrologically by Kosco (1981). Progress reports touching on our own intermittent work at Trident were summarized in Hildreth (1987, 1990), Fierstein and Hildreth (2000), and Hildreth and Fierstein (2000).

Basement Rocks

Quaternary volcanoes of the Katmai cluster are built atop a rugged set of glaciated ridges carved from subhorizontal to gently warped marine siltstone and sandstone (fig. 4) of the Jurassic Naknek Formation (Riehle and others, 1993; Detterman and others, 1996). These well-stratified rocks are intruded locally by porphyritic granitoid stocks of Tertiary age. Although both types of basement rock crop out as high as 4,500 ft (1,370 m) near the col between Trident and Mount Katmai (fig. 3), the Trident lavas drape and conceal most of the basement down to elevations no higher than 2,600 ft (790 m) to the southeast and 1,500 ft (460 m) to the south. At the western and northern margins of the Trident group, where

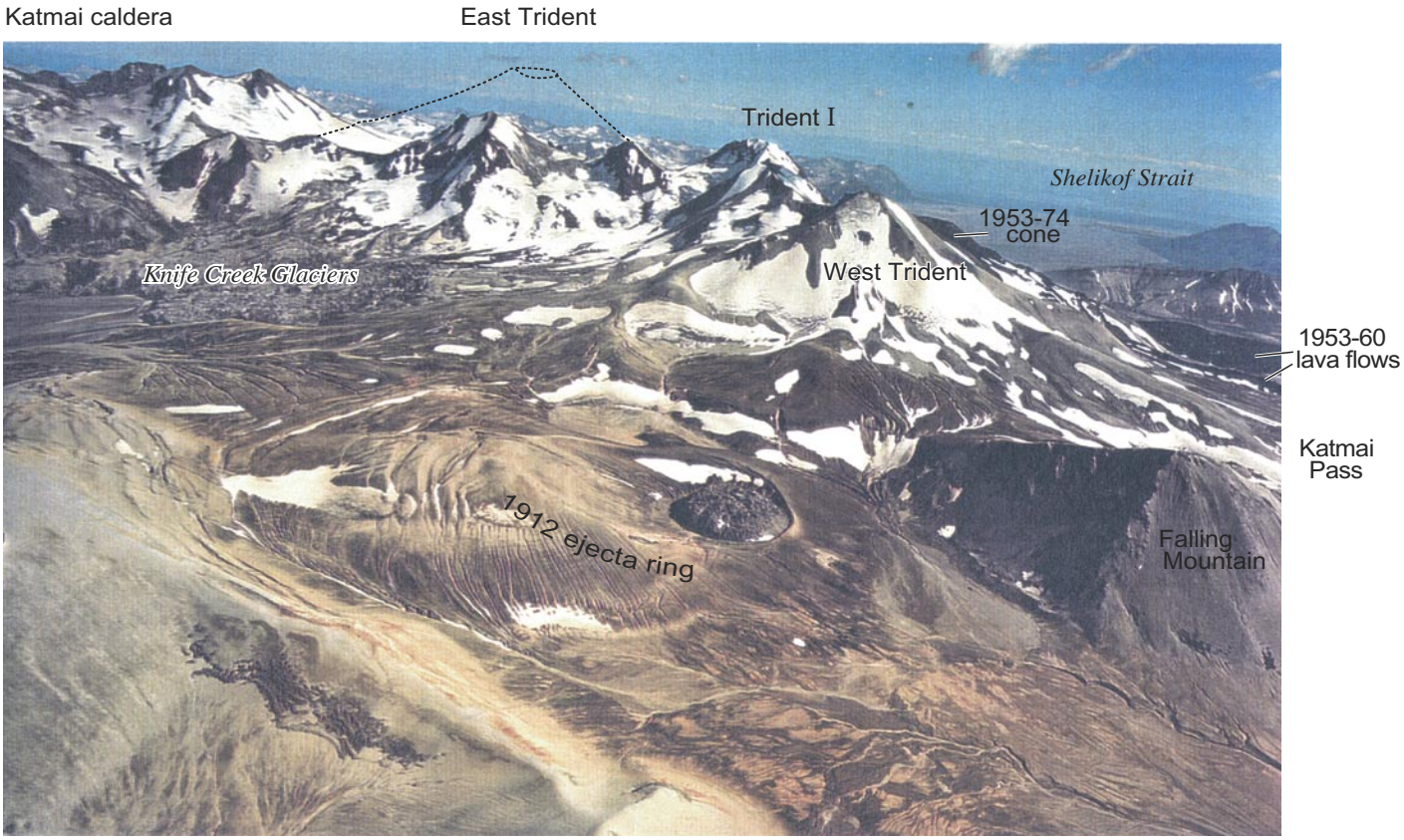

Figure 2. Aerial panorama of Trident Volcano southeastward over 1912 vent depression and small circular lava dome, Novarupta, in central foreground (see fig. 1 for locations). At upper left, Katmai caldera (centered 10 km east of Novarupta) is separated by a low saddle from four prominent peaks of the Trident group. Eastern two peaks are glaciated remnants of East Trident Volcano (as schematically reconstructed); highest is Trident I Volcano, and 3 km behind Novarupta is snowclad West Trident Volcano. Partly hidden behind West Trident is black cone of Southwest Trident (1953–74) and its lava-flow apron (at far right) in Katmai Pass and Mageik Creek. Flat in distance is alluvial plain of Katmai River, which joins Shelikof Strait at Katmai Bay. On blue horizon beyond strait is Kodiak Island. Foreground is dominated by 1912 vent depression, which extends 2.5 km northeastward (to left) from base of 400-m-high scarp of Falling Mountain dacite dome (lower right), a member of the Trident group. 1912 vent funnel was backfilled by welded ignimbrite and fallback ejecta, deformed by compaction-induced faulting, and plugged by 380-m-wide Novarupta rhyolite dome, which is surrounded by a strongly asymmetric ejecta ring. Low gray lobes in left middle distance at foot of East Trident and Mount Katmai are Knife Creek Glaciers, still covered by 1912 ejecta.

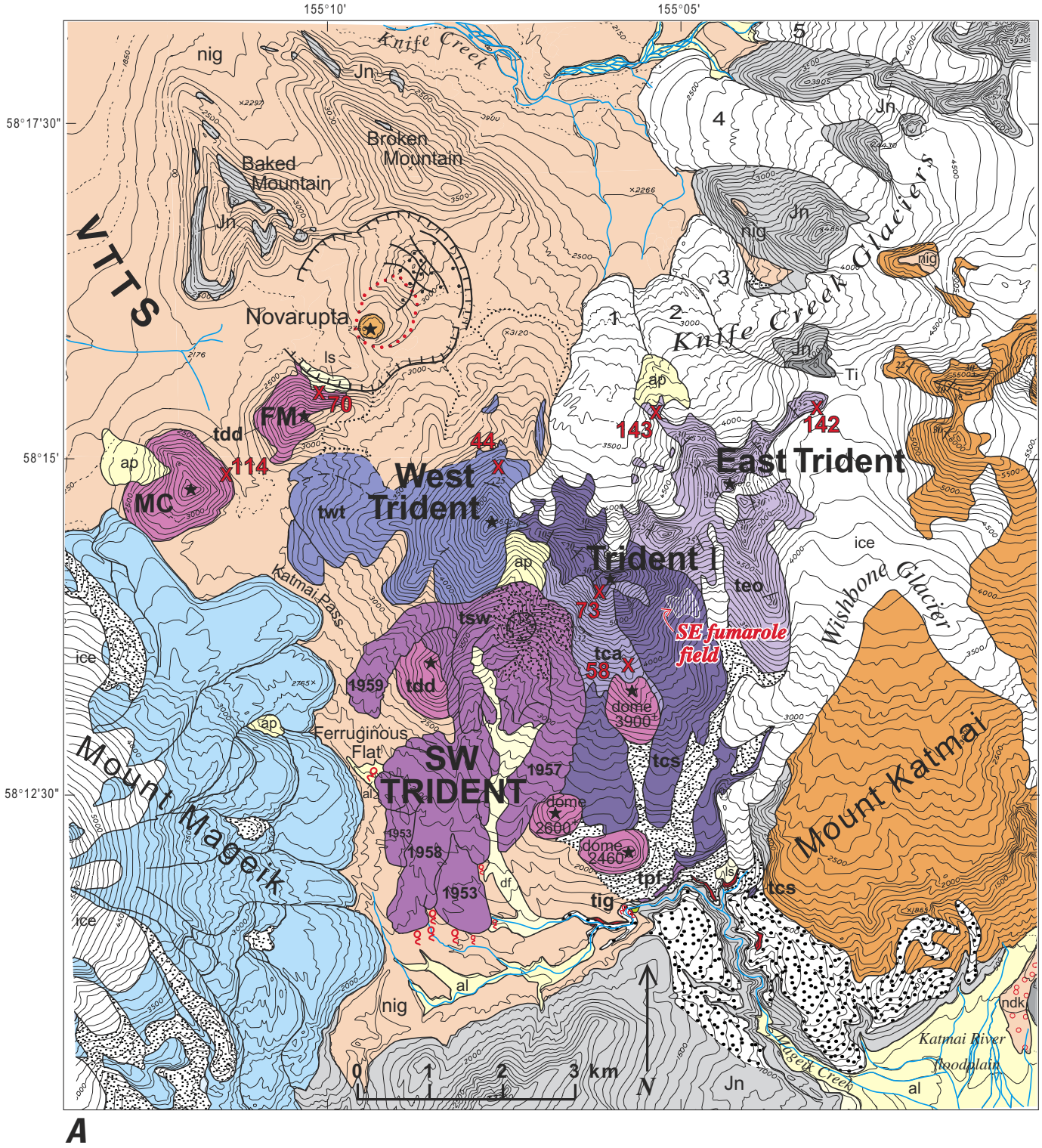

Figure 3. Geologic and topographic maps of the Trident group, flanked by Katmai and Mageik Volcanoes, southern Alaska (see fig. 1 for locations). *A*, Simplified geologic map. To north is the Valley of Ten Thousand Smokes (VTTS), floored by 1912 ignimbrite (unit nig), which also flowed through Katmai Pass from vent at Novarupta (hachured depression) into upper basin of Mageik Creek. Main Trident cones are labeled, and their three-letter unit labels (tca, tcs, teo, tsw, twt) are explained in text. Year of emplacement is labeled for principal lava flows of Southwest Trident, outline of which is drawn from aerial photographs atop preeruptive 1951 topography. Site of initial 1953 outbreak was beneath present crater (hachures) but was subsequently buried by incremental growth of fragmental cone (stippling). Six Trident lava domes (unit tdd) are distinguished, two largest of which are Mount Cerberus (MC) and Falling Mountain (FM). Along Mageik Creek canyon, unit tig (tiny, in green, due south of dome 2460) is dacitic ignimbrite remnant, and unit tpf is lithic pyroclas-

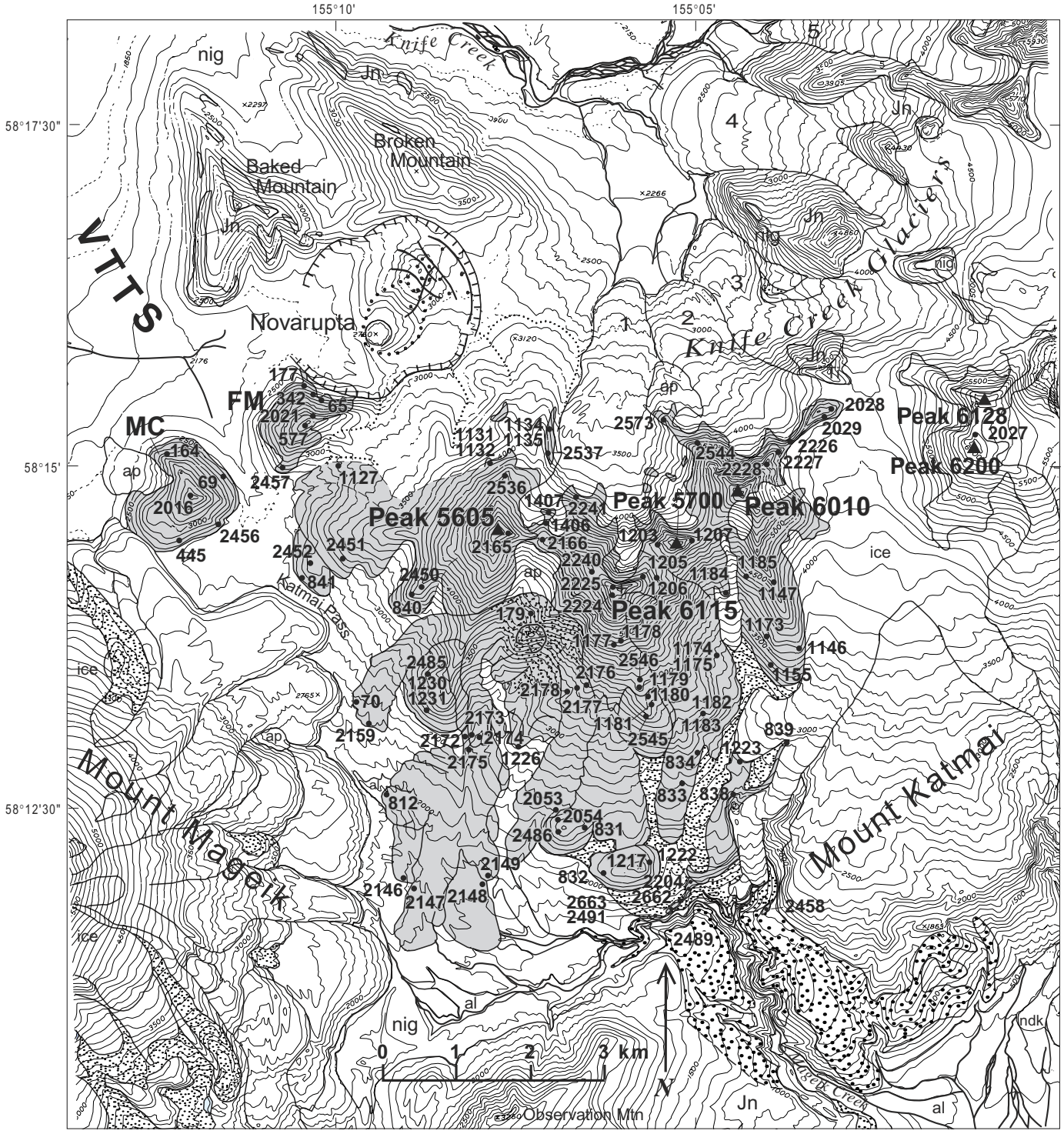

B

tic-flow deposit; both units are Trident derived. Nearby remnants (red areas) are canyon-wall exposures of late Pleistocene rhyodacitic plinian pumice fall and ignimbrite from Mount Katmai. Coarse stippling, Pleistocene till; finer stippling, Holocene till. Bold red Xs, locations of dated samples, with ages in thousands of years (ka). Red tadpoles denote clusters of warm springs. Jn, Jurassic basement rocks of the Naknek Formation; ndk, Katmai River debris-flow deposit of 1912 (Hildreth, 1983); Ti, Tertiary granitoid intrusion. Surficial deposits (pale yellow): al, stream alluvium; ap, pumiceous alluvium reworked from 1912 deposits; df, debris-flow deposits of remobilized ejecta from Southwest Trident cone; ls, landslide and rockfall rubble. *B*, Topographic map of Trident group, showing locations of samples listed in tables 1 and 2 (with K– prefixes omitted) and a few key elevations (in feet). Topographic base for both panels from U.S. Geological Survey 1:63,360-scale Mount Katmai A–4 and B–4 quadrangles (1951); contour interval, 100 ft.

1912 pyroclastic deposits completely obscure any Trident-basement contacts, the subvolcanic basement configuration is poorly known, although it might be as high as 2,500 ft (760 m) in Katmai Pass where thoroughly concealed by 1912 material. Remnants of Tertiary or early Quaternary andesite-dacite volcanic rocks are common just east of Mount Katmai (Riehle and others, 1993), but none are exposed near the Trident group, the products of which are observed (fig. 4) or inferred (fig. 3) to lie directly on the Naknek Formation.

Although Permian to Jurassic sedimentary rocks that regionally underlie the Naknek Formation (itself more than 2 km thick) do not crop out in the Katmai area, the stratigraphic framework of the Alaska Peninsula (Detterman and others, 1996) suggests that such rocks are as much as 3.5 km thick beneath the Katmai volcanoes.

The Mesozoic basement rocks upon which the volcanic centers are built belong to a tectonostratigraphic package commonly called the Peninsular terrane, which is widely thought to have originated far to the south and to have been added to southern Alaska during the middle and late Mesozoic (Plafker and others, 1994). Since then, several additional terranes and subduction-related accretionary complexes were added along Alaska's southern margin, such that the Aleutian Trench (5–6 km below sea level) now lies 350 km southeast of the volcanic line. Eocene sea floor is currently being subducted here, nearly orthogonally, at a convergence rate of about 6 cm/yr. The inclined seismic zone is well defined and 20 to 30 km thick (Kienle and others, 1983). It dips only about 10° NNW. for some 300 km, then steepens to about 45° beneath the present-day arc, and persists to depths as great as 200 km; its top lies about 100 km beneath the Katmai volcanic cluster. Although the arc alignment shifted modestly during the Tertiary (Wilson, 1985; Riehle and others, 1993), the Aleutian Arc was well established along the Alaska Peninsula by the middle Eocene, soon after the onset of northwestward motion of the Pacific Plate beneath southern Alaska (Plafker and others, 1994). The present-day volcanic front trends rather linearly N. 65° E. along the Katmai segment of the arc (fig. 1).

Although the crust beneath the modern volcanic chain remains immature and is probably only 30 km thick, it can be considered at least quasi-continental because many Tertiary

Figure 4. Trident group from the south, with gorge of Mageik Creek in foreground (figs. 1, 3). Stratified rocks on canyon walls are marine siltstone and sandstone of the Jurassic Naknek Formation, dipping 10° ESE. (to right). On skyline at left is black cone of Southwest Trident (1953–74), which largely conceals West Trident edifice, top of which is visible through the adjacent saddle. High central edifice is Trident I (peak 6115), summit lava of which yields an age of 73±12 ka. Two skyline peaks at right are both parts of East Trident edifice, altered core of which has been excavated into a large cirque, still partly occupied by ice. Dark ledge at center is pumice-covered andesitic lava flow from Trident I, forming canyon rim. Steep scree at right descends from buttress of andesitic lava flows erupted at Mount Katmai. Lavas of both Trident and Katmai rest directly on strata of the Naknek Formation. View northward.

granitoid plutons have invaded the Peninsular terrane basement. Crustal earthquakes, generally shallower than 10 km, are abundant beneath the Katmai volcanoes (except Mount Griggs). As many as 1,000 local earthquakes each year have recently been recorded here by the Alaska Volcano Observatory, nearly all of them of $M<2.5$ (Ward and others, 1991; Jolly and McNutt, 1999; Power and others, 2001).

East Trident

The two eastern peaks of the Trident group (figs. 2–4) are both remnants of East Trident Volcano (unit teo, fig. 3), a small andesite-dacite stratocone (58–65 weight percent SiO_2) almost contiguous with Mount Katmai. The rugged edifice is exposed over a 3- by 4-km area, but its lower flanks are concealed beneath glaciers. The hydrothermally altered core of East Trident is gutted by five glacial cirques excavated into the edifice, exposing on steep glacial headwalls windows of stratified ejecta deep in the interior of the skeletal cone. The ridges between cirques reveal structurally simple stacks of 10 to 25 radially dipping lava flows and breccia sheets (fig. 5), mostly silicic andesite, 8 to 30 m thick, but the 100-m-thick lava flows that support the southwest ridge and part of the northeast ridge are dacite (63–65 weight percent SiO_2). The northeast-ridge dacite, which is stratigraphically high in the pile and extends nearly to the summit (peak 6010), yields a K-Ar age of 142±15 ka. An analytically indistinguishable age of 143±8 ka for a near-basal andesitic lava flow low on the northwest ridge suggests, however, that activity at the small East Trident cone was short lived, late in the middle Pleistocene. These ages also indicate that East Trident is the oldest edifice of the Trident group and is, indeed, older than neighboring Katmai and Mageik Volcanoes, as well. Peak 5700+, central prong of the "Trident" as seen from the south or southeast (fig. 4)—the aspect that inspired the name—is not a separate cone but a west-dipping remnant of the ruggedly eroded southwest flank of East Trident. Reconstruction suggests that the cone may once have exceeded 6,600 ft (2,010 m) in elevation (fig. 2), probably making it the highest of the Trident summits.

Figure 5. East Trident Volcano, with upper Glacier 3 and northwest buttress of Mount Katmai in foreground (figs. 1, 3). Radial stacks of thin rubbly andesitic lava flows and breccias that dip east (to left) and northwest (to right) support skyline ridges. Central ridge descending from sharp summit (peak 6010) is likewise a stack of andesitic-dacitic lavas, which dip northeast (toward observer) and end in pumice-mantled buttress at center. Adjacent to top of steep glacier on east face, pale-colored acid-altered rocks on skyline form rim of volcano's glacially gutted core, which is occupied by another cirque on far side of edifice (see fig. 4). Pumice-covered ridge at right consists of nonvolcanic basement rocks; ice-fringed ridge in left foreground consists of andesitic lava flows from Mount Katmai. On right skyline, snowy Mount Mageik forms backdrop 8 km beyond saddle separating West Trident (far right) from Trident I (largely hidden). View southwestward.

Trident I

Likewise sculptured glacially, Trident I (peak 6115) is a discrete andesitic cone (53–63 weight percent SiO_2) that forms the central and highest edifice (6,115 ft [1,864 m]) of the Trident group. Its lavas apparently bank against East Trident at their (poorly exposed) mutual saddle, but some overlap of their active lifetimes is not excluded by our present data. Buttressed by East Trident on its northeast, the Trident I edifice (units tcs, tca, fig. 3) grew asymmetrically toward the other sectors. The core of the Trident I edifice is eviscerated by a north-face cirque (fig. 6), the sheer headwall of which reveals the base of the vertically jointed 150-m-thick summit lava (63 weight percent SiO_2), which rests on more than 200 m of crudely stratified coarse breccia. This dacitic lava may be a dome remnant that overlies crater fill and dome breccia on its north side. On its southwest side, the summit dacite rests on a coherent andesitic lava flow (61.7 weight percent SiO_2) that yields a K-Ar age of 73±12 ka. The northwest ridge of the edifice consists mostly of a glaciated stack of thinner lava flows and breccias, but low on steep northern spurs of the ridge are two massive andesitic lavas (60 weight percent SiO_2), each 100 to 200 m thick, which are probably glacially truncated coulees but, alternatively, might be older domes.

The smoother, less dissected south slope of Trident I (fig. 4) consists largely of summit-derived andesitic lava flows (58–62 weight percent SiO_2) and poorly exposed block-and-ash flows that descend to elevations as low as 1,500 ft (450 m) at Mageik Creek. In contrast, the southwest slope (fig. 7) is made up of steeply dipping (25°–35°) sheets, 0.1 to 3 m thick, of agglutinated mafic fallout rich in accidental lithic fragments, subordinate thin pyroclastic-flow deposits, and associated avalanche rubble. Derived from the central vent of Trident I, these deposits (unit tca, fig. 3) are generally gray brown to brick red, but parts were altered ocherous yellow or orange brown, probably while still hot. Fresh juvenile scoriae and spatter in these deposits are olivine-rich andesite, the most mafic material (53–55 weight percent SiO_2) known to have been erupted from the Trident group. A dense spatter blob from agglutinate on the south slope gave a $^{40}Ar/^{39}Ar$ plateau age of 58±15 ka (Hildreth and others, 2003). The strata also contain abundant accidental clasts of the pyroxene andesite that makes up most of the edifice.

Although the edifice of Trident I is glacially ravaged and has had no Holocene eruptions, its lower southeast flank is marked at 3,600- to 4,000-ft (1,100–1,220 m) elevation by a field of sulfur-depositing fumaroles, first recorded in 1916 by Griggs (1922, p. 98) and still vigorous. Another fumarole,

Figure 6. Cirque headwall forming north face of Trident I (peak 6115, figs. 1, 3). Relief framed is 450 m (1,500 ft). Craggy dacitic lava on summit, probably a dome remnant, rests on andesitic lava that yields an age of 73±12 ka and overlies massive and stratified breccia that dips 20°–30° NW., forming cliff at right, which is northeast face of northwest ridge of edifice. Andesite knob (elev, 5,700 ft) on right skyline is draped by buff 1912 pumice-fall deposit. View southward from helicopter.

visible on 1951 aerial photographs as a 100-m-wide steaming pit at 3,850-ft (1,175 m) elevation on the southwest ridge of Trident I, became the vent site for the new volcanic cone that began to grow in 1953 (see section below entitled "Southwest Trident").

West Trident

West Trident (peak 5605) is the smallest and youngest of the prehistoric Trident edifices, as well as the one closest to Novarupta (fig. 2). Heavily mantled by 1912 fallout, its lavas (unit twt, fig. 3) are poorly exposed except near the summit (fig. 8) and along the west wall of Glacier 1. All lavas exposed are silicic andesite or dacite (58–64.4 weight percent SiO_2), and many are unusually rich in chilled enclaves (1–20-cm diam) of phenocryst-poor, relatively mafic andesite (54–58 weight percent SiO_2). The summit lava (61 weight percent SiO_2), which is nearly 100 m thick, may be part of a dome (fig. 8). Adjacent lava flows dip 20° down the north ridgeline (fig. 8), and the top one thickens downslope to 70 m. Other summit-derived lavas and breccia sheets dip east against Trident I at their mutual saddle. Although the contact is obscured by 1912 and 1953 pyroclastic deposits, the contrast between these east-dipping silicic andesite flows and the steeply southwest-dipping sheets of mafic agglutinate that make up the nearby southwest face of Trident I supports the inference (based on physiography and attitudes of lavas) that West Trident is truly a discrete cone rather than a shoulder of Trident I isolated by erosion. The K-Ar age of 44±12 ka measured for the thick andesitic lava flow that forms the crest of the north ridge (fig. 8) supports our stratigraphic and morphologic inference that West Trident is the youngest of the prehistoric centers in the Trident group.

Mostly ice free today, West Trident was formerly ice covered and is everywhere glacially modified. On its flanks, poorly exposed glaciated lavas form an array of seven sharp-crested ridges that descend radially from the summit. Four northerly spurs and the southwest ridge all appear to be lava flows, but the west and south ridges may include lava domes abutted by lava flows from West Trident and later jointly sculptured glacially and blanketed by 1912 pumice falls. Some of the northerly lava flows bank against Falling Mountain dome (70±8 ka), and just east of there the distal parts of adjacent lavas were destroyed on June 6, 1912, by collapse into the

Figure 7. Southwest face of Trident I edifice (figs. 1, 3). Entire left slope, as well as dark buttress to right of pumice scree chute, is composed of steeply dipping sheets of agglutinate, scoria, and breccia (58±15 ka) that largely consist of olivine-rich andesite (53–55 weight percent SiO_2), most mafic material identified in Trident group. Much of mafic material is altered, especially on orange-brown to ocher lower slopes. Pumice-mantled knob on left skyline (elev, 5,700 ft; also visible in fig. 6) is a stratigraphically higher andesitic lava flow (60.4 weight percent SiO_2) that dips 20° NW. down northwest ridgeline, away from observer. Craggy skyline unit at right is dacite dome on summit of Trident I (see figs. 4, 6). View northward from helicopter.

Novarupta vent, thereby providing most of the andesitic lithic clasts among the Episode I ejecta (Fierstein and Hildreth, 1992).

Trident Domes

At least five (and as many as eight) pyroxene-dacite lava domes (62–65 weight percent SiO_2) line the lower west and south flanks of the Trident group (unit tdd, fig. 3). Three ambiguous candidates along Katmai Pass are steep blunt-nosed buttresses of West Trident that were abutted or overrun by younger lava flows, sculptured glacially, and so heavily mantled by 1912 pyroclastic deposits that their distinction as domes or thick flow lobes from West Trident remains uncertain. These eight domes do not include the four domes (or thick proximal flows) already mentioned high on the adjacent edifices of Trident I and West Trident. All 12 domes lie within 7 km of each other in a compact zone that includes the site of the new cone built in 1953–74.

The two largest domes (fig. 9), 425-m-high Falling Mountain and 365-m-high Mount Cerberus (each 0.3–0.4-km^3 volume), are compositionally similar to the smaller (unnamed) domes, which range in volume from 0.015 to 0.12 km^3. Like West Trident, all the domes contain chilled enclaves (1–15-cm diam) of phenocryst-poor andesite (54–58 weight percent SiO_2), although such enclaves are uncommon in the dacite of Mount Cerberus. All the domes are glacially scoured, and several are severely eroded. Mount Cerberus and Falling Mountain, however, are stout domes that are morphologically little modified by ice and were suspected of being very young (Hildreth, 1983, 1987). Repeated search has nonetheless turned up few remnants of glassy carapace, and K-Ar data now give late Pleistocene ages for both domes—Falling Mountain 70±8 ka and Mount Cerberus 114±46 ka. The superficiality of glacial erosion may reflect their compact profiles and positions close to the Alaska Peninsula drainage divide. Flanking the entrance to Katmai Pass at the northwest foot of West Trident (fig. 9), both domes (63–65 weight percent SiO_2) have a compositional affinity (low K, Zr) with the Trident group. A lava flow from the East Summit subedifice of Mount Mageik banks against Mount Cerberus, and lavas from the West Trident cone bank against Falling Mountain (fig. 3). The northeast face of Falling Mountain was destroyed during the great eruption at Novarupta (fig. 2), providing some of the accidental lithic clasts in 1912 pyroclastic deposits (Fierstein and Hildreth, 1992).

Two low domes (2460 and 2600+) on the north side of Mageik Creek are glacially subdued, abutted by lava flows from Trident I and Southwest Trident, and heavily mantled by 1912 fallout (fig. 10). Each has only 150 m relief and a volume of 0.030 to 0.035 km^3, in contrast to dome 3900+ (2 km farther north, fig. 10), which has twice the relief and 3 times the volume. All the domes have clear compositional affinity (low K, Zr) with the Trident group and are chemically and

Figure 8. Northeast face of West Trident Volcano (peak 5605, figs. 1, 3). Steep face provides only large exposure on edifice, which is elsewhere blanketed by thick 1912 fallout from nearby Novarupta. Three andesitic lava flows dip to right, down north ridge; top flow yields K-Ar age of 44±12 ka. Face-forming lava, 70 to 100 m thick, which dips toward observer and into saddle separating West Trident from Trident I, may be a thick lobe of an otherwise-concealed summit dome. In foreground, andesitic lava flow capping northwest ridge of Trident I edifice dips northwest beneath West Trident edifice. View westward.

Figure 9. Falling Mountain and Mount Cerberus dacite domes, from the River Lethe on floor of the Valley of Ten Thousand Smokes (figs. 1, 3). In background, summit of snow-streaked West Trident (peak 5605) is in cloud. At left, Falling Mountain rises 430 m above valley floor, and at right, Mount Cerberus rises 365 m. Together they frame the entrance to Katmai Pass. Both domes are heavily mantled with 1912 pyroclastic deposits from Novarupta, which lies out of view, just left of Falling Mountain (see fig. 2). View southeastward.

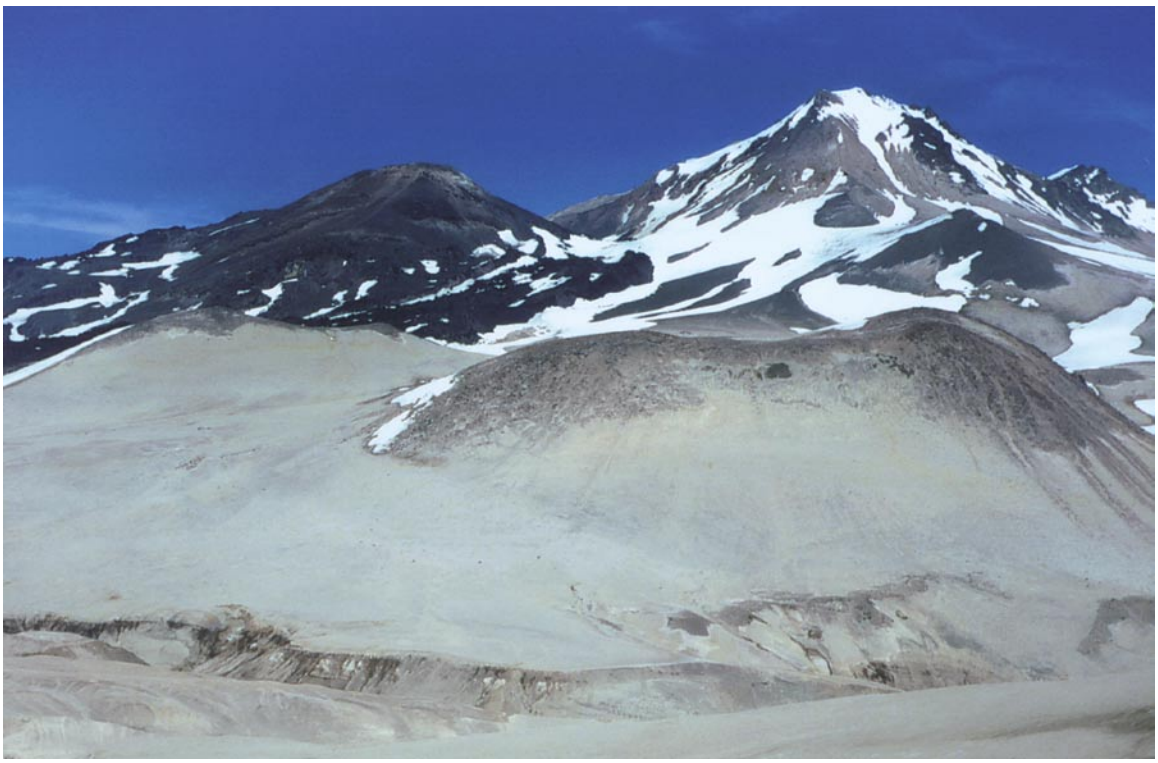

Figure 10. Three glacially eroded dacite domes south of Trident I (snow-streaked summit edifice) and Southwest Trident (1953–74 black cone at upper left), with Mageik Creek at foot of Observation Mountain in foreground (figs. 1, 3). Saddle-shaped dome 2460 (62–63 weight percent SiO_2) in right foreground and, to its left, dome 2600+ (64–65 weight percent SiO_2) are heavily blanketed by 1912 pumice-fall deposits. At right center, dome 3900 (63.5 weight percent SiO_2) forms black triangular spur on midslope of Trident I. View northward.

petrographically similar to summit domes and thick coulees on West Trident and Trident I. Except for Falling Mountain and Mount Cerberus, none of the domes has been dated, but all are glacially eroded, and each is older than one or more contiguous lava flows from West Trident or Trident I. Attempts to date one of the domes failed twice, probably because it is too young to have accumulated measurable radiogenic Ar. The likelihood is that all the peripheral domes were extruded during the late Pleistocene, evidently contemporaneously with growth of the adjoining composite cones, Trident I and West Trident.

Pyroclastic-Flow Deposits

The many domes and thick lava flows of dacite and silicic andesite that typify activity at Trident I and West Trident suggest that numerous block-and-ash flows (hot pyroclastic flows that carry mostly nonpumiceous juvenile clasts) would have been shed during construction of those edifices. However, glaciers have removed most pre-Holocene unconsolidated material around the base of the Trident group, and thick 1912 pyroclastic deposits cover the entire apron except along the canyon of Mageik Creek. There, in several protected alcoves along the winding gorge, which is cut as deeply as 150 m into Jurassic basement rocks (fig. 4), remnants of pyroclastic deposits from both Trident and Mount Katmai are interbedded with glacial and proglacial deposits.

A nonwelded dacitic ignimbrite (pumiceous pyroclastic-flow deposit) crops out on the south wall at the upper end of the gorge of Mageik Creek, due south of Trident I (unit tig, fig. 3). The greenish-gray massive remnant, 7 m thick and only 35 m long, rests on Jurassic strata a few meters above stream level (fig. 11). The lithic-poor unconsolidated deposit is rich in 1- to 5-cm-diameter pumice clasts and has a median grain size of 1.3 mm, and its sandy matrix is relatively poor in fine ash (only 6 weight percent finer than 63 μm). Although the deposit is a single massive emplacement unit, slight size sorting of pumice clasts imparts a hint of vague layering that etches out on weathered surfaces. The dominant greenish-gray to black pumice is dacitic (63–64 weight percent SiO_2), but subordi-

Figure 11. Nonwelded dacitic ignimbrite remnant (unit tig, fig. 3*A*) on south wall of upper end of Mageik Creek gorge, due south of Trident I and dome 2460 (figs. 1, 3, 10). Single greenish-gray massive outcrop, 7 m thick and 35 m long (at center, behind 1.625-m geologist), rests on and banks against Jurassic basement rocks (lower left) a few meters above stream level. Lithic-poor tuff is rich in small (1–5-cm diam) pumice clasts. Predominant greenish-gray to black pumice is dacitic (63–64 weight percent SiO_2), but subordinate white pumice is rhyodacitic (70–71 weight percent SiO_2). Compositional affinity of all pumice types is clearly with Trident group (relatively low K and Zr contents), not with Mount Mageik or Mount Katmai, but composition fails to distinguish among Trident I, West Trident, and Trident domes as likely source of these pumiceous pyroclastic flows. Deposit is overlain directly by 3 m of boulder-rich till, capped by about 10 m of 1912 pumice falls and fines-rich ignimbrite, which provides tan mud dribbling down wall.

nate white pumice is rhyodacitic (70–71 weight percent SiO_2). Compositional affinity of all pumice types is clearly with the Trident group (low K, Zr), not with Mount Mageik or Mount Katmai, but composition fails to distinguish among Trident I, West Trident, or Trident domes as the likely source. Because the ignimbrite is directly overlain by a single sheet of bouldery till only a few meters thick (fig. 11), which is, in turn, capped only by 1912 deposits, we infer that it was emplaced very late in the Pleistocene. Because the ash flow was funneled along the gorge at a level 30 m lower than the base of lithic pyroclastic-flow unit tpf, described next, this ash flow is almost certainly younger.

A block-and-ash-flow deposit (fig. 12) is preserved as inset remnants in four alcoves high on the north wall of Mageik Creek gorge at the south foot of Trident I (unit tpf, fig. 3). Its gray sandy matrix encloses black to medium-gray, dense glassy juvenile clasts, mostly 1 to 10 cm but as much as 50 cm across, as well as abundant nonjuvenile clasts of varied andesite and dacite. Disregarding clasts coarser than 16 mm, sieve analysis shows the matrix to have a median grain size of 5 mm, with only 1.5 weight percent finer than 63 μm. The four main exposures range in thickness from 10 to 30 m, but the deposit is largely eroded away between adjacent alcoves. The alcove farthest downstream contains the coarsest and thickest deposit, which consists of several flow units and could represent more than one eruptive event. All four remnants are overlain by thin layers of till and fluvial gravel, probably representing only the last Pleistocene glacial advance, and all rest on Jurassic basement rocks or on fluvial deposits that overlie the basement rocks. The deposit is cut by numerous clastic dikes, possibly induced by the stress of overriding ice. A total of 12 glassy clasts analyzed range in SiO_2 content from 57.6 to 71.8 weight percent, a strikingly wide compositional variation that constitutes a notable anomaly, because no other sample from the Trident group has yielded more than 65.5 weight percent SiO_2 (except the white pumice in unit tig). The compositional affinity of all blocks analyzed, however, is clearly with the Trident group (low K, Zr), not with Mount Mageik or Mount Katmai. Composition does not distinguish among Trident I, West Trident, or the Trident domes as a likely source of the pyroclastic flows.

Figure 12. Block-and-ash-flow deposit preserved as inset remnants high on north wall of Mageik Creek gorge (unit tpf, fig. 3*A*), just southeast of dome 2460. Dark-gray deposit, here 20 m thick, consists of several flow units defined by zones of coarse clasts. At lower right, deposit rests on Jurassic strata, which dip gently southeast (to right). Dark-gray sandy matrix encloses black to medium-gray, dense glassy clasts as much as 50 cm across (but mostly 1–10-cm diam), as well as varied nonjuvenile andesite-dacite clasts (rarely as large as 1-m diam). Although glassy clasts vary widely in composition (63–72 weight percent SiO_2), compositional affinity of all blocks analyzed is unequivocally with the Trident group (relatively low K and Zr), not with Mount Mageik or Mount Katmai. White and tan slopes in background are covered by scree of 1912 pumice, which conceals till, talus, and fluvial gravel that overlie pyroclastic-flow deposit. View eastward, downstream along north rim of gorge.

Also preserved locally along the gorge of Mageik Creek are remnants of a major rhyodacitic plinian pumice-fall and nonwelded ignimbrite deposit (71–72 weight percent SiO_2). Its compositional affinity is with Mount Katmai, not Trident. Organic material at the base of the fallout yields a radiocarbon age of 19,240±70 ^{14}C yr B.P., equivalent to a calibrated calendar age of 22.8 ka (Hildreth and Fierstein, 2000). Pertinent here is that mutual canyon-filling relations along Mageik Creek indicate (but do not conclusively prove) that the Katmai-derived deposit predates both Trident-derived pyroclastic-flow deposits just described (units tig, tpf, fig. 3). If so, both Trident-derived units are constrained to have been emplaced during the long interval of fitful glacial retreat—between the Last Glacial Maximum (approx 21 ka) and final withdrawal to typical Holocene termini (by approx 8 ka).

Finally, on the south apron of Trident I, a sharp south-flowing gully just southeast of dome 3900+ cuts through thick 1912 fallout and 2 m deeper into a subjacent block-and-ash-flow deposit containing enclave-rich andesite blocks, as much as 50 cm across. The uniformly oxidized, purplish-brown, sandy matrix of the deposit encloses abundant dense clasts of plagioclase-rich pyroxene andesite (61.4 weight percent SiO_2), either segregated into lenses or fully matrix supported. Clearly derived from Trident I, the flow was probably not associated with extrusion of the summit dome, which is dacitic (63.4 weight percent SiO_2), but rather with one of the contiguous near-summit lavas, several of which consist of silicic andesite (60.4–62.2 weight percent SiO_2). Because it lacks the rhyodacite clasts present in the block-and-ash-flow deposit only 1.5 km farther south at Mageik Creek (unit tpf, fig. 3), this poorly exposed flow unequivocally represents a separate eruption.

Southwest Trident

Beginning in February 1953, a new andesite-dacite edifice (0.7-km^3 volume) was built at the southwestern margin of the Trident group (unit tsw, fig. 3). Though sometimes referred to informally as "New Trident," we have called it Southwest Trident (Hildreth and others, 2000), in anticipation of the day it ceases to be Trident's youngest component. During 2 decades of sporadic explosive activity (Vulcanian type and effusive), a new composite cone covering about 3-km^2 area was constructed of block-and-ash deposits, scoria, agglutinate, stubby lava lobes, and the intercalated proximal parts of the main lava flows that spread as an apron beyond the cone. The cone grew to an elevation of 4,970 ft (1,515 m) (Global Positioning System measurement by Coombs and others, 2000) on the former site of a 100-m-wide fumarolic pit at about 3,840-ft (1,170 m) elevation on the steep southwest flank of

Figure 13. Southwest Trident in July 1979 (5 years after cessation of eruptive activity), from Mount Mageik (figs. 1, 3). Dark-gray-brown pyroclastic cone, disposed asymmetrically on slope of glaciated Trident lavas, rises 750 m above Katmai Pass in foreground. Shallow summit crater is 350 m wide. Leveed 1959–60 lava flow is visible at left, and overlapping flows of 1953 and 1958 at lower right (see fig. 3); just beyond them, snow-filled trough marks western margin of 1957 flow, which extends past right edge of photograph. Rounded tan knob wrapped by young flows at lower center is snout of glaciated ridge of West Trident lava (visible in fig. 15*A* before it was overrun). Summits of West Trident and Trident I edifices are in cloud at upper left. Upper Katmai River and Shelikof Strait are visible at upper right. View eastward.

Trident I. Although relief on its south slope exceeds 700 m (fig. 13), the new cone thus has a central thickness of only 345 m and a volume of about 0.3 km^3. At successive stages of cone construction, four blocky leveed lava flows effused from its central vent, in 1953, 1957, and 1958 and during the winter of 1959–60 (figs. 3, 13). Each flow is 25 to 60 m thick and 2.5 to 4 km long, and altogether they add about 0.35 km^3 to the eruptive volume. The cone's summit is today marked by a shallow crater, 350 m wide (fig. 14), that was the site of several small ephemeral plugs, which were emplaced after the final lava flow and were repeatedly destroyed by intermittent explosive activity (1960–74).

Black, rapidly expanding, cauliflower ash clouds rose 6 to 9 km at least 10 times between 1953 and 1974 and possibly 12 km once or twice. Several times during the first month of activity, light ashfall dusted areas as far as 30 to 50 km from the vent, in all sectors. By far the most voluminous fallout appears to have resulted from the initial outburst of February 15, 1953 (Snyder, 1954), which may have been sub-Plinian. A single nongraded scoria-fall layer (5–17 cm thick) deposited during that event is preserved at a few protected sites as far away as Mount Katmai and upper Knife Creek. Sieve data for bulk samples of this layer yield median and maximum particle sizes, respectively, of 6.5 and 100 mm in the saddle 1 km north of the vent, and 2.1 and 20 mm in the saddle 7 km northeast of the vent—between the twin western summits of Mount Katmai. Thin sheets of finer ash that fell during the many smaller subsequent outbursts have been almost entirely removed or reworked by wind and runoff. Abundant ballistic blocks, variously bread-crusted, densely vitrophyric, or scoriaceous, that are scattered as far as 3 km from vent are products of many discrete explosive episodes (none of which were closely observed) distributed over 2 decades. Liberal estimates of total fallout volume yield no more than 0.05 km^3, contributing less than 10 percent of the total eruptive volume of 0.7±0.1 km^3.

The period of most frequent observation was from February to September 1953, principally by military reconnaissance aircraft during the early months (Snyder, 1954) and by a U.S. Geological Survey (USGS) party that camped at Knife Creek during the summer (Muller and others, 1954). When the vent was first seen through the cloud layer on the fourth day of activity (Feb. 18, 1953), an effusive lava flow (then already

Figure 14. East to northeast face of Southwest Trident cone in July 1997, from near summit of Trident I (figs. 3, 4). Visible cone material includes agglutinate sheets and unconsolidated stratified ejecta, covered downslope by apron of blocky scree. Primary deposits are mostly coarse but poorly sorted; blocks range in texture from dense to scoriaceous. Lava flows visible in figure 13 emerge from other side of cone. Few remaining fumaroles and little alteration mark interior of 350-m-wide crater, which was site of several plugs of dense lava, repeatedly destroyed. On outer slopes just below rim, however, hundreds of sulfurous fumaroles emerge through permeable ejecta, promoting alteration of 100-m-wide light-colored zone. In the 1960s, many of these fumaroles were still superheated, but the hottest measured in 1997 was only 95°C. In background, Holocene lava flows from Mount Mageik are overlain by pale-gray 1912 pumice-fall deposit. View southwestward.

250 m wide) was upwelling centrally and spreading radially (fig. 15*A*). Although a fumarolic pit, as much as 40 m deep, was conspicuous at the impending ventsite on aerial photographs taken in 1951 (and had probably been further excavated by the explosive outburst of Feb. 15), any such crater was soon filled and buried by the effusive lava (fig. 15*A*), which continued to be extruded and spread slowly throughout the seven months of intermittent observation in 1953. At various times, lava lobes emerged laterally through the chilled carapace at the foot of the pile, or the pile itself "expanded like a balloon" and extruded lobes by overflow from the vent, or small slumps and slide masses detached from the steep flow margins (Snyder, 1954). By June 1953, the main southerly tongue of lava, ultimately 4.2 km long, had advanced only 1,250 m from the vent. Snyder (1954) estimated the volume of fallout and lava produced by June 17, 1953, at 0.23 to 0.3 km^3, about a third of the eventual output. During the summer, steady steaming and continued spreading of the lava was punctuated sporadically by steam bursts (fig. 15*B*) or occasional "smoke columns" that rose 1 to 3 km and dusted various proximal sectors with minor additional ashfall (Muller and others, 1954).

Observations after September 1953 were sporadic and few. A general chronology of major events was compiled by Decker (1963) and augmented by Ray (1967), largely from intermittent National Park Service reports. The 1953 lava flow may not have attained its final dimensions (fig. 3) until early 1954 or later. Apparently, no observations were made

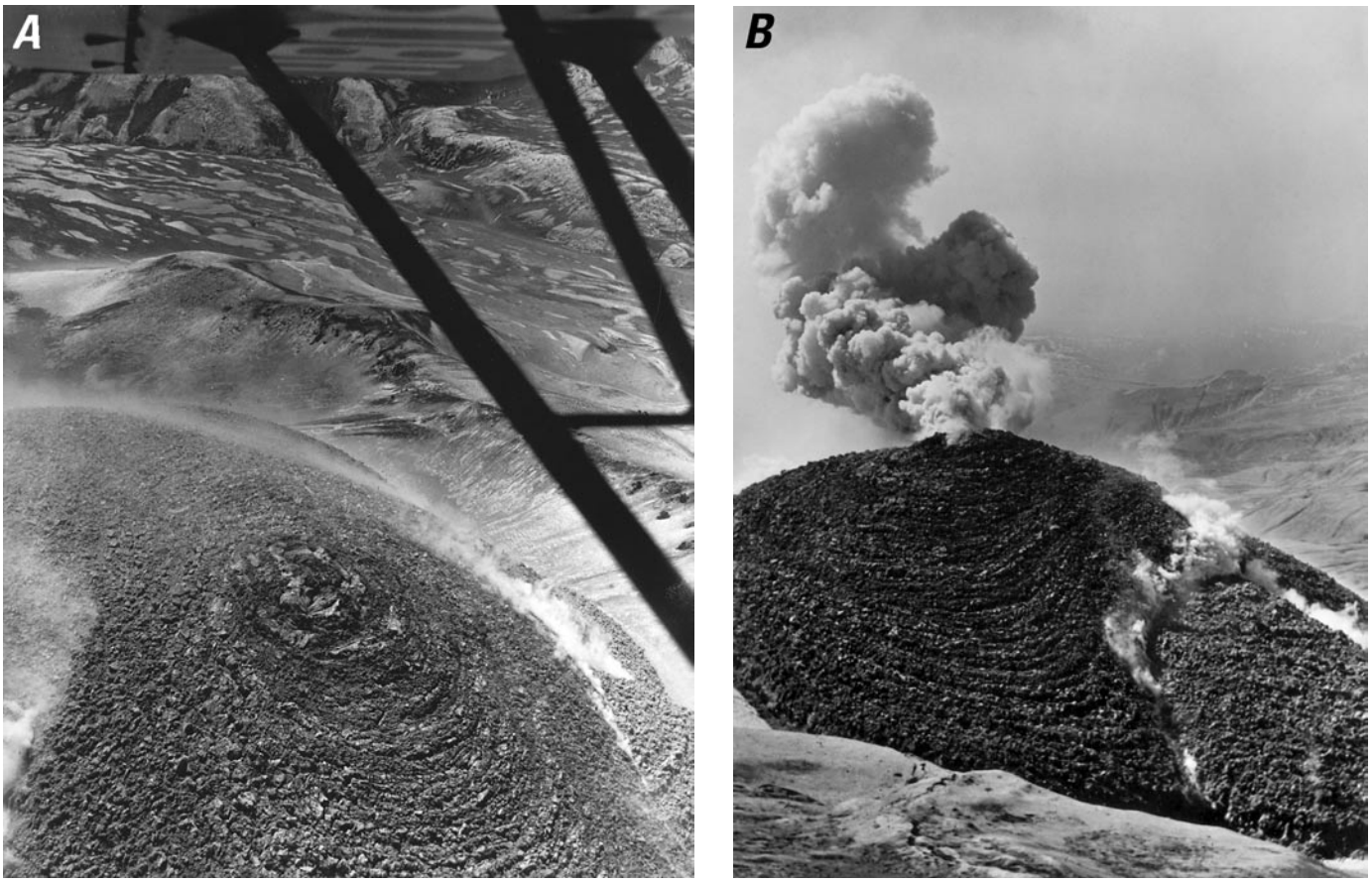

Figure 15. Transient vent configurations at Southwest Trident in June 1953 (figs. 1, 3). *A*, Concentric corrugations around orifice of initial andesite lava flow from Southwest Trident, about 4 months after initiation of 1953 eruption. Note absence of crater at focus of upwelling. Asymmetric outflow of effusive lava is partly toward observer but principally southward (to upper left). In background, streaks and patches of thin black ash that overlie light-colored 1912 pumice falls and ignimbrite were deposited as fallout, mostly during initial explosive events of February 1953. By June 1953, much of the black ash had already been reworked by wind and runoff, and by the time of our first visit in August 1976, nearly all of it had been removed. Lava visible here was completely covered by subsequent 1953–60 lava flows and by growth of a pyroclastic cone over vent. Ridge of glaciated lava crossing middle of photograph was also largely covered later, except that its rounded terminus remains exposed as a dome-shaped hump wrapped by younger flows (figs. 3, 13). Andesite-dacite coulees from Mount Mageik are visible in distance. View southwestward; National Park Service photograph taken by Garniss H. Curtis, June 1953. *B*, Same concentrically corrugated pile of effusive andesite surrounding vent in figure 15*A*, showing a small burst of steam and ash and a fissure-bounded lateral effusion on northwest flank. View southward from saddle north of vent; National Park Service photograph, taken by Garniss H. Curtis, June 1953.

during eruption and outflow of the lava flows of 1957, 1958, and 1959–60 (fig. 3), merely aerial snapshots taken in the summer seasons after the emplacement of each flow. The time of emplacement of the lava flow attributed to the winter of 1959–60 is the least well known, because no photographs are known to have been taken between September 1958 and August 1960. The 1958 lava flow partly overran the 1953 flow (fig. 3) and impounded a small lake on upper Mageik Creek that soon filled in with pumiceous alluvium, becoming a mudflat (Ferruginous Flat, fig. 3) now marked by numerous iron-precipitating warm springs.

Growth of the fragmental cone (figs. 13, 14) began only after much or all of the 1953 lava flow (fig. 15) had been emplaced. The cone accumulated progressively during the later 1950s, as shown by emergence of the successive lava flows at different levels of the fragmental edifice. National Park Service photographs show that the cone had attained nearly its full height by 1960, although explosive showers of blocks continued to augment the cone until 1974. In addition to the four main lava flows, cone construction included emplacement of several stubby lava lobes limited to its proximal southwest slope (fig. 3). The southeast side of the cone completely buried a 1-km^2-area cirque glacier, with no recognized effects on eruptive behavior or edifice structure, although enhanced steaming may have contributed to the stronger fumarolic emission and alteration on that side of the cone (fig. 14). Explosive ejections of tephra, some involving blowout of plugs and at least one spine, took place from 1960 to 1974, but volumetrically significant eruptions were over by 1963. Numerous sulfurous fumaroles, superheated in the 1960s but below and at the boiling point today, persist on the upper parts of the cone (fig. 14). Dark-gray bouldery debris flows reworked from the pyroclastic deposits have built a proximal fan and thin distal sheets (1–4 m thick) that cap stream terraces for 3 km downstream along Mageik Creek. Some debris flows resulted from the initial February 1953 fallout over snow, and others from avalanching of rubble from the steep slopes of the cone.

The lava flows and ejecta are olivine-poor two-pyroxene andesite and dacite that span a compositional continuum from 56 to 65.5 weight percent SiO_2. All products are plagioclase rich and contain 33 to 45 volume percent phenocrysts, many of them complexly zoned, resorbed, and overgrown (Ray, 1967; Kosco, 1981; Coombs and others, 2000). The least evolved bulk material identified is the initial scoria fall of February 1953 (56–57 weight percent SiO_2). Andesitic enclaves are abundant, relatively mafic (56–59 weight percent SiO_2), contain the same phenocryst species as the host material, and fall mostly in the size range 1–30 cm (Coombs and others, 2000). No evidence of contamination by leftover 1912 magma (such as quartz phenocrysts) has been found, and small but consistent compositional differences (Hildreth and Fierstein, 2000) indicate that the andesitic-dacitic magmas erupted in 1912 and in 1953–74 were different batches. For the Southwest Trident batch, Coombs and others (2000) presented experimental and analytical evidence for mixing between resident dacitic magma stored at 890°C at about 3-km depth and a newly arrived batch of 1,000°C andesitic magma; they interpreted diffusion profiles in phenocrysts to suggest that thorough mixing could have produced the linear compositional array within about a month before the eruption began.

Geochronology

K-Ar ages were determined on whole-rock samples from some of the lava domes and from each of the three main glaciated edifices of the Trident group (table 1); sample-selection criteria and analytical methods were described by Hildreth and Lanphere (1994) and Lanphere (2000). Seeking high-precision ages for late Pleistocene rocks, we used the multiple-collector mass spectrometer (Stacey and others, 1981) at the USGS laboratory in Menlo Park, Calif.

On stratigraphic grounds, the three glaciated cones of the Trident group appear to young westward, because each cone is buttressed by its eastern neighbor. This observation is borne out by the K-Ar data because the East Trident edifice yields the oldest ages and West Trident the youngest.

For East Trident, a near-basal andesitic lava flow resting on oxidized breccia at glacier level on the nose of the northwest prong (which separates Glaciers 1 and 2, fig. 3) yields a weighted mean age of 143±8 ka, analytically indistinguishable from an age of 142±15 ka on a 100-m-thick dacitic lava flow that caps part of the northeast ridge of the edifice. These samples appear to bracket most of the dozens of lava flows that make up the edifice, suggesting that eruptive activity at the small East Trident cone was short lived. The ages indicate not only that East Trident is the oldest member of the Trident group but also that it predates the oldest recognized eruptive products of neighboring Katmai and Mageik Volcanoes (Hildreth and Fierstein, 2000; Hildreth and others, 2000).

An andesitic lava flow that directly underlies the summit dome of Trident I, about 100 m southwest of peak 6115, yields an age of 73±12 ka. Most of the edifice appears to lie stratigraphically beneath this lava, except for the mafic pyroclastic assemblage (unit tca, fig. 3), which apparently drapes many of the andesites and yields a $^{40}Ar/^{39}Ar$ age of 58±15 ka (Hildreth and others, 2003). Because much of the Trident I pile is banked against its eastern neighbor (dated at 143±8 ka), the active lifetime of Trident I appears to be reasonably well bracketed.

For West Trident, which banks against Trident I, a 70-m-thick andesitic lava flow capping the north ridge gave a K-Ar age of 44±12 ka. An attempt to date the summit lava of West Trident (fig. 8) failed to yield sufficient radiogenic Ar to provide a meaningful age, supporting our field inference that it is still younger than the dated lava flow.

Falling Mountain dacite dome, the northeast face of which was sheared off (fig. 2) during the 1912 eruption at adjacent Novarupta, yields an age of 70±8 ka. Adjacent Mount Cerberus, a compositionally similar dacite dome (fig. 9), yields a less precise age of 114±46 ka, which (in view of the

Table 1. Whole-rock K-Ar ages and analytical data for Trident Volcano.

[Analysts: K by D.F. Siems; Ar by F.S. McFarland and J.Y. Saburomaru. Constants: $\lambda=0.581\times10^{-10}$ y^{-1}, $\lambda_\beta=4.962\times10^{-10}$ y^{-1}, $^{40}K/K=1.167\times10^{-4}$ mol/mol]

Sample (table 2)	Location (fig. 3)	SiO_2 (wt pct)	K_2O (wt pct)	Radiogenic ^{40}Ar		Calculated age (ka)
				(10^{-13} mol/g)	(pct)	
K–2573	East Trident: near-basal lava flow on nose of NW. ridge.	60.0	1.069±0.001	2.144	7.2	139±12
				2.279	8.7	148±12
				weighted	**mean---**	**143±8**
K–2029	East Trident: 100-m-thick dacitic lava flow capping NE. ridge.	65.1	1.657±0.006	3.380	3.9	142±15
K–2224	Trident I: thick lava flow at 6,000 ft; 100 m SW. of summit 6115.	61.7	1.348±0.008	1.960	6.4	73±12
K–2536	West Trident: thick lava flow capping north ridge at 4,500 ft.	62.1	1.403±0.003	.891	1.8	44±12
K–65	Falling Mountain: north spur.	65.0	1.759±0.004	1.763	8.0	70±8
K–69	Mount Cerberus: east face.	63.0	1.300±0.002	2.130	2.1	114±46

respective analytical errors) need not differ significantly from that of Falling Mountain.

Eruptive Volumes

The glaciated East Trident edifice today covers an area of about 7 km^2, Trident I about 15.2 km^2, and West Trident about 12.6 km^2. The eastern and northern aprons of East Trident, however, have been covered and largely removed by glaciers, and its original summit, crater, and altered core have been glacially gutted. The same is true for the core and northern apron of Trident I. The southern apron of Trident I is glacially scoured but not incised, thus relatively intact, although any former intracanyon flows along Mageik Creek have been stripped. West Trident has not been excavated so severely, but its summit and radial ridges are everywhere ice scoured, and its apron lavas were truncated distally by ice that flowed across Katmai Pass. Moreover, its northern lava-flow apron was truncated by the 1912 Novarupta vent depression, and the rest largely concealed by 1912 pyroclastic deposits, more than 10 m thick. Attempting to estimate original volumes of the edifices is therefore a difficult and uncertain exercise.

Although the summits of all three Pleistocene cones were at times ice covered, the observation that remnants of summit domes seem to have survived on Trident I and West Trident suggests that neither cone has been reduced in elevation by more than 100 m. From the attitudes of stratified ejecta and lavas that compose the radial arêtes of East Trident, however, we infer that its summit has been lowered by about 200 m (fig. 2).

Reconstructions based on the observations and assumptions just outlined yield preerosion edifice volumes of 6 to 8 km^3 for East Trident, 7 to 9 km^3 for Trident I, and 3 to 4 km^3 for West Trident, to which can be added 0.7 km^3 for the 1953–74 products of Southwest Trident and about 1 km^3 for the peripheral lava domes. The pyroclastic-flow deposits preserved along the gorge of Mageik Creek are unlikely to have contributed as much as another 1 km^3, but the remnants are in any case too few to allow meaningful reconstructions. With the possible exception of these pyroclastic-flow deposits, no eruptive unit has been observed in the Trident group that is likely to have been accompanied by a cubic-kilometer-scale explosive pyroclastic deposit subsequently lost to erosion. Regional fallout ejected during explosive phases of andesitic or low-silica dacitic eruptive episodes like those at Trident seldom amount to more than a few tenths of a cubic kilometer, as observed during the 1953–74 activity, which produced less than 0.1 km^3 of such fallout. We thus arrive at a total eruptive-volume estimate for the Trident group of about 21±4 km^3, which can be compared to 30 km^3 each for nearby Mageik and Griggs Volcanoes and to 45 km^3 for the compound edifice of Mount Katmai (excluding its far-flung tephra deposits).

Because the oldest eruptive products exposed in the (still active) Trident group yield an age of 143±8 ka, the reconstructed volume of 21±4 km^3 yields a long-term average eruption rate in the range 0.11–0.18 km^3/k.y.—greater than that of

nearby Snowy Mountain, similar to that of Mount Griggs, only a third that of Mount Mageik, and barely a tenth that of Mount Katmai (Hildreth and others, 2000, 2001, 2002, 2003; Hildreth and Fierstein, 2000, 2003).

Composition of Eruptive Products

Chemical analyses of 116 samples representing all components of the Trident group are plotted in figure 16 and listed in table 2. Sample suites for all volcanoes in the Katmai cluster, including Trident, show broadly similar, low-Ti, medium-K calc-alkaline arc trends (Gill, 1981) that are mutually distinguishable on variation diagrams by only a few element pairs. For example, the variation trends of Al, Ti, Ca, Na, Rb, Ba, Mg, and Fe plotted against SiO_2 substantially overlap for all main-chain volcanoes from Mount Martin to Snowy Mountain (fig. 1). A fair separation of several of the suites is provided, however, by variation patterns of K_2O, Zr, and Sr against SiO_2, as shown in figures 8 through 10 of Hildreth and Fierstein (2000). The key compositional differences (K_2O, Zr) that distinguish magmatic products of the Trident group from those erupted at adjacent Novarupta are plotted in figures 16*A* and 16*C*.

Alkali-lime intersections for Trident data arrays fall at 63.5 weight percent SiO_2 (fig. 16*B*), defining calcic suites by the index of Peacock (1931). The 1912 Novarupta suite and products of all the Katmai centers on the main volcanic line are likewise calcic, in contrast to the calc-alkalic suite erupted at Mount Griggs (Hildreth, 1983; Hildreth and others, 1999, 2001, 2002). By the Fe-enrichment criterion of Miyashiro (1974), however, all the compositional arrays in the Katmai cluster (including those of Trident and Mount Griggs) are strongly calc-alkaline (non-tholeiitic).

Primitive magmas have not erupted at any of the Katmai volcanoes. Although mafic magmatic inclusions (enclaves) in andesitic lavas throughout the cluster contain as little as 54 to 57 weight percent SiO_2, only at Trident I (table 2) and Snowy Mountain (Hildreth and others, 2001) have mafic products been identified that contain more than 7 weight percent MgO. At Trident, such Mg-rich compositions are restricted to the sheeted agglutinate that makes up the upper southwest slope of Trident I. Apart from a few enclaves that contain 5.0 to 5.35 weight percent MgO, no other Trident lavas or ejecta have been found to contain as much as 5 weight percent MgO.

We previously showed that the continuously zoned andesite-dacite suite erupted at Novarupta in 1912 was withdrawn from beneath Mount Katmai (Hildreth, 1991) and that the suite has a closer compositional affinity to the eruptive products of Mount Katmai than to those of other volcanoes in the cluster (Hildreth and Fierstein, 2000). Eruptive products of East Trident, oldest edifice in the Trident group and close neighbor of Mount Katmai, are distinguishable from those of Novarupta and Mount Katmai in their relatively lower contents of both Zr and K_2O (fig. 16). Trident I, West Trident, and the peripheral domes are likewise consistently deficient in Zr and K_2O relative to the Katmai-Novarupta array, and higher Sr contents distinguish them from East Trident (Hildreth and Fierstein, 2000). The data thus indicate that all pre-1953 constituents of the Trident group were supplied by magma reservoirs physically separate from those that fed Mount Katmai and Novarupta. The compositional similarity of Falling Mountain and Mount Cerberus to West Trident and the other Trident domes likewise confirms that the magmatic affinity of those dacite domes lies with the prehistoric Trident group, not with adjacent Novarupta.

Uniquely among the several components of Trident, the 1953–74 products of Southwest Trident are close to being compositionally collinear with those of Katmai and Novarupta on most variation diagrams (fig. 16). The Southwest Trident suite is nonetheless distinguishable by its slightly lower K_2O and Fe and slightly higher Na and Sr contents relative to the 1912 array (Hildreth and Fierstein, 2000). The most evolved 1953–74 material analyzed contains 65.5 weight percent SiO_2 (Coombs and others, 2000), and only a few samples contain more than 63 weight percent SiO_2 (table 2; Ray 1967; Kosco, 1980). In contrast, the 4.5 km^3 of dacite that erupted in 1912 was zoned to 68 weight percent SiO_2, and most of it contained more than 65 weight percent SiO_2 (fig. 16). No xenocrystic evidence has been observed in 1953–74 material for contamination by leftover (quartz bearing) 1912 rhyolite, and there is no hint in the 1953–74 andesite-dacite array of a mixing trend toward the (Zr deficient) 1912 rhyolite (Hildreth and Fierstein, 2000).

We conclude that the andesitic-dacitic magma that built Southwest Trident was similar, but not identical, to the 1912 andesitic-dacitic magma that drained from beneath Mount Katmai to the Novarupta vent at the toe of West Trident (figs. 2, 3). The 1953–74 dacite probably occupied a shallow reservoir near Katmai Pass, physically remote from that of 1912. The dacitic reservoir may have been disturbed by andesitic replenishment during the decade or so preceding 1951, the year when fumaroles were first observed on the subsequent site of Southwest Trident. Major andesitic replenishment may not have stimulated thorough convective mixing with the resident dacitic magma until a month or so before the eruption began in February 1953, as suggested by the mixing and diffusion-profile data of Coombs and others (2000). Compositional similarities are consistent, however, with the interpretation that the andesitic batches involved in the 1912 and 1953 eruptions were ultimately supplied by the same deep-crustal reservoir.

The Pleistocene pyroclastic-flow remnants south of the Trident group (figs. 11, 12, 16) require additional comment. All 16 samples from three different eruptive units (table 2) fall well below the 1912 Novarupta arrays on the K_2O and Zr panels (fig. 16). As illustrated in Hildreth and Fierstein (2000), these compositional constraints unequivocally eliminate nearby Mageik and Katmai Volcanoes as the sources of the pyroclastic flows, leaving the Trident group as the only possible source. The data (fig. 16; table 2) show that the block-and-ash-flow deposit (sample K–833) poorly exposed on the south flank of Trident I is compositionally similar to several lava flows high on that edifice. However, juvenile

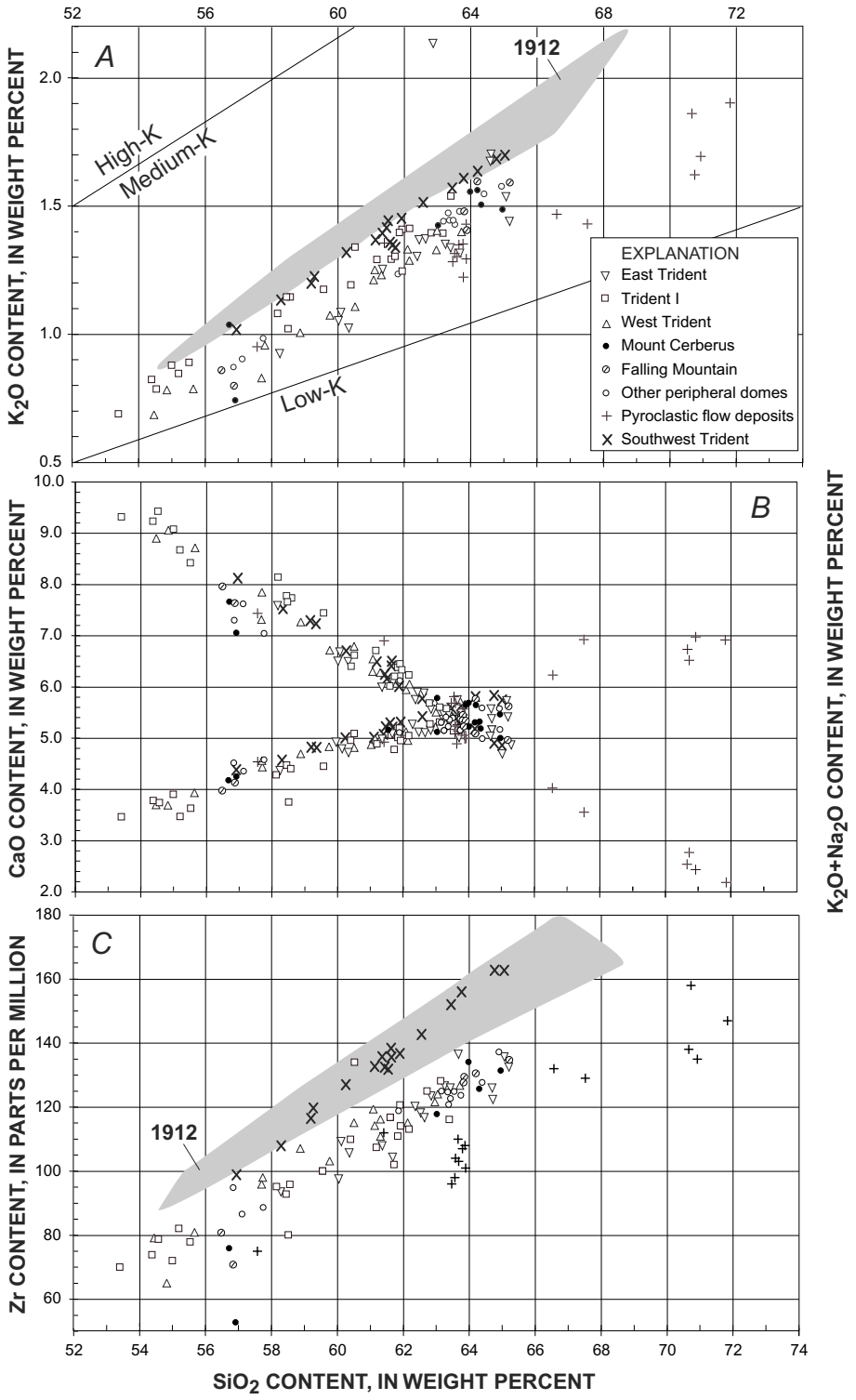

Figure 16. Whole-rock compositional data for 116 samples from Trident group, subdivided as in inset. Sample sites are shown in figure 3*B*, and data are listed in table 2. *A*, K_2O versus SiO_2 contents. *B*, CaO (upper trend) and total alkalies (lower trend) versus SiO_2 contents. C, Zr versus SiO_2 contents. For comparison, shaded fields show continuous compositional arrays for about 200 samples of zoned andesite-dacite suite erupted from Novarupta in June 1912 (Hildreth and Fierstein, 2000). Suite erupted in 1953–74 at Southwest Trident is compositionally closer to 1912 array than is any older component of Trident group. Anomalously high-Zr Trident I sample is from 200-m-thick lava, lowest unit exposed at base of north face. Anomalously high-K East Trident sample is from window of flow breccia beneath wasting ice tongue that separates south ridge of edifice from southeastern fumarole field. Note that most samples of pyroclastic flows plot below main arrays in figures 16*A* and 16*C*.

Table 2. Chemical analyses of eruptive products from Trident Volcano.

[Wavelength-dispersive X-ray-fluorescence analyses of major-element oxides in weight percent, normalized to H_2O-free totals of 99.6 weight percent (allowing 0.4 weight percent for trace-element oxides and halogens); energy-dispersive X-ray-fluorescence analyses of minor elements (Rb, Sr, Zr) in parts per million. Analyst, D.F. Siems, U.S. Geological Survey laboratory, Lakewood, Colorado. Precision and accuracy of these measurements were discussed by Baedecker (1987) and Bacon and Druitt (1988). FeO*, total Fe calculated as FeO; LOI, percentage of sample weight lost on ignition at 900°C; original total, volatile-free sum of major-element-oxide contents before normalization, with total Fe content calculated as Fe_2O_3. Suffix "–i" on sample number denotes magmatic enclave included in a host lava. See figure 3 for sample locations and lithologic units]

Sample (fig. 3)	SiO_2	TiO_2	Al_2O_3	FeO*	MnO	MgO	CaO	Na_2O	K_2O	P_2O_5	LOI	Original total	Rb	Sr	Zr
East Trident															
K–1146	60.32	0.75	16.82	7.23	0.14	2.96	6.51	3.72	1.03	0.14	0.50	98.90	22	309	106
K–1147	63.22	.76	15.98	6.27	.14	2.20	5.47	4.05	1.36	.15	1.01	98.46	25	257	127
K–1155	62.45	.65	16.37	6.08	.12	2.75	5.90	3.78	1.38	.13	.24	99.20	30	271	119
K–1173	62.63	.65	16.39	6.02	.12	2.62	5.89	3.75	1.38	.14	.54	99.07	29	273	117
K–1184	62.86	.71	16.27	6.22	.13	2.44	5.60	3.06	2.14	.18	2.09	97.33	27	273	124
K–1185	61.35	.74	16.53	6.99	.10	2.71	6.02	3.75	1.26	.14	2.58	96.43	22	275	109
K–1203	60.09	.77	16.82	7.07	.15	3.00	6.70	3.76	1.09	.14	<.01	99.45	21	293	110
K–1207a	63.39	.65	16.39	5.77	.10	2.34	5.47	3.99	1.34	.15	2.19	96.63	25	280	125
K–1207b	58.25	.71	17.21	7.36	.14	3.82	7.59	3.46	.93	.13	<.01	99.52	16	294	94
K–2028	63.65	.81	16.52	5.50	.13	1.99	5.04	4.44	1.32	.21	.37	98.90	22	291	137
K–2029	65.06	.66	15.86	5.21	.12	1.98	4.80	4.20	1.55	.16	<.01	99.20	31	265	136
K–2226	61.67	.70	16.36	6.42	.13	2.89	6.13	3.77	1.36	.18	1.04	98.03	19	291	105
K–2227	64.68	.61	15.88	5.20	.12	2.25	5.09	3.88	1.70	.19	1.81	96.93	30	258	126
K–2227r	64.68	.61	15.85	5.27	.12	2.34	5.16	3.72	1.69	.16	1.92	97.13	29	251	123
K–2228	65.17	.60	15.87	5.10	.12	2.20	4.95	4.00	1.45	.16	1.25	97.75	30	256	133
K–2573	60.00	.78	16.65	7.25	.14	3.12	6.52	3.87	1.06	.21	.38	98.82	18	306	98
K–2574	62.39	.69	16.22	6.28	.13	2.61	5.78	3.97	1.31	.22	.00	99.17	24	297	120
Trident I															
K–834	59.57	0.67	16.78	6.46	0.12	3.97	7.44	3.28	1.18	0.13	0.51	99.14	25	338	100
K–834–i	54.39	.78	17.86	7.93	.14	5.35	9.24	2.95	.82	.14	.96	99.26	18	400	74
K–838	58.18	.65	16.92	6.64	.13	4.53	8.13	3.20	1.08	.13	.18	99.46	21	357	95
K–839	61.90	.60	17.38	5.44	.11	2.41	6.45	3.92	1.25	.13	.50	99.11	28	310	121
K–1174	61.93	.65	16.52	6.06	.11	2.92	6.33	3.54	1.41	.12	.40	98.91	28	308	114
K–1175–i	54.99	.78	18.20	8.05	.15	4.33	9.07	3.03	.88	.12	.68	98.52	16	393	72
K–1177	58.50	.87	17.83	6.08	.15	4.58	7.71	2.73	1.02	.14	3.92	95.51	18	372	80
K–1178	53.41	.91	18.69	8.86	.17	4.57	9.33	2.78	0.69	.19	1.32	98.04	10	417	70
K–1179	55.20	.64	16.42	7.58	.14	7.34	8.67	2.63	0.85	.14	.85	98.60	15	241	82
K–1182	61.85	.64	16.60	5.92	.12	2.95	6.38	3.62	1.40	.12	0.87	98.39	27	309	111
K–1183–i	54.53	.79	18.24	8.00	.14	4.60	9.43	2.95	.79	.13	.65	98.82	19	409	79
K–1205	61.18	.64	16.62	6.14	.12	3.16	6.71	3.60	1.29	.13	<.01	99.47	30	309	107
K–1206	62.17	.63	16.44	5.94	.12	2.90	6.24	3.63	1.41	.12	.01	99.33	25	302	113
K–1223	58.57	.70	16.65	6.78	.13	4.47	7.73	3.26	1.15	.17	.01	99.50	19	340	96
K–1406	63.11	.65	16.45	5.63	.12	2.58	5.61	3.91	1.39	.15	.03	99.26	25	321	128
K–1407	62.81	.68	16.32	5.91	.13	2.68	5.64	3.88	1.40	.15	–.02	99.14	22	320	125
K–2166	61.61	.69	16.71	6.15	.13	3.03	6.03	3.77	1.29	.18	.07	98.98	23	332	117
K–2224	61.72	.68	16.65	6.16	.13	3.09	6.21	3.47	1.30	.18	2.28	96.71	19	294	102
K–2225	63.41	.62	16.21	5.55	.11	2.62	5.58	3.80	1.54	.16	.34	98.62	29	295	116
K–2240	60.39	.72	16.87	6.54	.13	3.39	6.41	3.75	1.19	.20	.00	98.87	21	341	110
K–2241	60.52	.74	16.70	6.39	.13	3.22	6.62	3.75	1.34	.19	–.09	99.30	28	311	134
K–2458	58.46	.69	16.64	6.71	.13	4.53	7.78	3.33	1.15	.19	–.01	99.22	20	360	93
K–2546	55.52	.63	16.35	7.54	.15	7.18	8.43	2.74	.89	.17	.83	98.12	17	237	78

Table 2. Chemical analyses of eruptive products from Trident Volcano—Continued

Sample (fig. 3)	SiO_2	TiO_2	Al_2O_3	FeO*	MnO	MgO	CaO	Na_2O	K_2O	P_2O_5	LOI	Original total	Rb	Sr	Zr
West Trident															
K–840	63.72	0.57	16.53	5.15	0.10	2.36	5.74	3.87	1.40	0.15	<0.01	99.41	28	320	127
K–840–i	57.69	.80	17.67	7.55	.17	3.68	7.32	3.73	.83	.17	<.01	99.79	15	393	96
K–841	58.88	.68	17.83	6.48	.13	3.48	7.27	3.69	1.01	.16	<.01	99.98	22	387	107
K–1127	61.30	.69	16.70	6.29	.13	3.05	6.30	3.74	1.23	.17	.09	99.38	23	332	116
K–1131	61.08	.66	16.70	6.24	.12	3.23	6.54	3.68	1.21	.15	.22	99.63	25	328	119
K–1132–i	55.64	.71	17.88	7.70	.14	4.74	8.71	3.15	.79	.14	.16	99.70	15	374	81
K–1134–i	57.71	.73	17.54	6.95	.13	4.09	7.85	3.49	.96	.16	<.01	99.93	20	398	98
K–1135	60.50	.68	17.00	6.19	.12	3.34	6.79	3.71	1.11	.15	<.01	99.59	24	346	115
K–2165	61.12	.68	16.76	6.33	.13	3.15	6.30	3.72	1.25	.17	.26	98.75	20	329	114
K–2450	62.96	.65	16.44	5.54	.12	2.75	5.73	3.88	1.33	.21	.01	99.23	22	312	122
K–2451	61.30	.68	16.55	6.25	.13	3.18	6.29	3.76	1.23	.22	–.04	99.21	22	320	111
K–2452	62.15	.67	16.52	6.00	.13	2.97	6.04	3.67	1.29	.17	.04	99.37	24	318	115
K–2452–i	54.84	.70	18.24	7.75	.15	5.04	9.05	2.91	.78	.14	.10	98.79	12	365	65
K–2536	62.09	.66	16.34	6.10	.13	3.00	5.97	3.77	1.33	.21	.02	99.47	22	338	115
K–2537	59.77	.74	17.14	6.51	.13	3.54	6.69	3.76	1.07	.24	–.11	98.87	15	374	103
Mount Cerberus															
K–69	63.02	0.65	16.14	5.82	0.12	2.73	5.78	3.74	1.43	0.17	0.15	99.48	26	281	118
K–164	63.98	.62	16.23	5.27	.10	2.34	5.23	4.13	1.56	.14	.18	99.12	31	297	134
K–164s	64.20	.63	16.29	4.96	.10	2.35	5.24	4.13	1.56	.13	– –	98.77	– –	– –	– –
K–445	64.95	.60	15.99	5.20	.11	2.11	5.01	4.02	1.49	.12	.13	99.06	29	285	132
K–2016	64.32	.64	16.01	5.42	.12	2.40	5.19	3.82	1.51	.18	.38	99.13	26	268	126
K–2456A–i	56.90	.85	17.52	8.58	.19	4.08	7.06	3.60	.74	.08	.10	98.97	13	353	53
K–2456B–i	56.72	.78	17.84	7.97	.16	4.14	7.67	3.14	1.04	.15	1.46	97.66	19	294	76
Falling Mountain															
K–177	64.19	0.62	16.22	5.20	0.10	2.20	5.15	4.19	1.60	0.13	0.31	98.59	30	299	131
K–372	63.83	.62	16.28	5.60	.12	2.31	5.47	3.82	1.41	.14	.00	99.09	25	321	129
K–577	65.17	.58	15.81	5.04	.11	2.13	4.98	4.05	1.59	.14	<.01	98.89	30	287	135
K–2021	63.79	.65	16.16	5.60	.12	2.38	5.35	3.88	1.48	.19	.00	99.54	23	311	128
K–2457A–i	56.48	.78	17.79	7.83	.16	4.45	7.96	3.13	.86	.17	.35	98.44	18	388	81
K–2457B–i	56.85	.84	17.92	7.78	.18	4.07	7.64	3.35	.80	.18	.25	98.38	16	378	71
Other peripheral domes															
K–831	64.93	0.54	16.58	4.61	0.10	1.93	5.17	4.00	1.58	0.16	0.36	99.10	22	298	137
K–832	61.87	.64	17.32	5.57	.11	2.66	6.14	3.88	1.24	.16	.15	99.48	31	352	119
K–832–i	56.85	.88	18.25	7.72	.14	3.79	7.31	3.61	.87	.18	.44	99.34	16	416	95
K–1180	63.52	.64	16.21	5.69	.12	2.55	5.40	3.91	1.43	.13	.04	98.93	33	293	125
K–1181–i	57.12	.76	17.67	7.74	.16	4.04	7.63	3.45	.90	.13	.10	99.22	18	360	87
K–1217	63.18	.69	16.29	5.79	.12	2.69	5.32	3.89	1.44	.18	.15	99.28	23	304	125
K–1230	62.99	.65	16.30	5.91	.13	2.71	5.51	3.83	1.41	.14	.31	98.98	25	280	124
K–1231–i	54.46	.77	18.26	8.20	.15	5.05	8.90	3.01	.69	.12	.64	98.75	15	379	79
K–2054	63.73	.66	16.36	5.51	.12	2.47	5.17	3.94	1.48	.17	.27	98.73	25	289	124
K–2054–i	57.74	.80	17.77	7.40	.13	3.94	7.05	3.61	.98	.18	.51	98.67	13	369	89
K–2485	64.40	.63	16.08	5.29	.12	2.27	5.01	4.05	1.55	.21	.17	98.57	30	279	128
K–2485A	63.36	.66	16.45	5.63	.12	2.53	5.24	3.93	1.45	.22	.88	98.44	24	282	121
K–2486	63.32	.67	16.34	5.64	.12	2.65	5.21	3.97	1.47	.22	.36	98.90	23	294	125
K–2545	63.42	.66	16.18	5.66	.13	2.55	5.38	3.97	1.44	.22	.11	98.78	24	293	123

Table 2. Chemical analyses of eruptive products from Trident Volcano—Continued

Sample (fig. 3)	SiO_2	TiO_2	Al_2O_3	FeO*	MnO	MgO	CaO	Na_2O	K_2O	P_2O_5	LOI	Original total	Rb	Sr	Zr
Pyroclastic-flow deposits															
Block-and-ash flow, Trident I:															
K–833	61.41	0.60	16.95	5.72	0.11	2.86	6.90	3.57	1.36	0.13	0.03	99.91	33	334	112
Pumiceous pyroclastic flow, Mageik Creek (unit tig):															
K–2489A	70.66	0.52	15.34	2.70	0.14	0.77	2.53	4.87	1.86	0.21	4.64	94.52	28	249	138
K–2489B	63.58	.82	16.46	5.33	.15	2.02	5.24	4.37	1.31	.31	2.41	96.57	21	313	104
K–2489C	63.89	.81	16.45	5.36	.16	1.99	5.00	4.34	1.29	.31	3.19	95.75	22	318	101
Lithic pyroclastic flows, Mageik Creek (unit tpf):															
K–1222	63.47	0.82	16.28	5.73	0.16	2.05	5.16	4.39	1.29	0.25	2.28	96.58	18	302	96
K–2204	63.56	.82	16.26	5.64	.16	1.99	5.09	4.50	1.31	.28	2.04	96.88	22	300	98
K–2204A	66.57	.73	15.88	4.43	.14	1.32	4.03	4.76	1.47	.26	.33	98.98	23	310	132
K–2204B	70.92	.50	15.08	2.67	.14	.73	2.44	5.28	1.69	.14	.34	98.84	26	246	135
K–2491A	67.52	.76	16.27	3.35	.09	.81	3.55	5.50	1.43	.31	.31	98.73	18	320	129
K–2491B	57.57	.99	16.75	8.57	.18	3.38	7.43	3.59	.95	.18	.70	98.44	15	334	75
K–2491C	71.83	.42	15.02	2.36	.14	.60	2.19	5.02	1.91	.13	1.52	97.34	32	239	147
K–2662A	70.73	.52	15.21	2.78	.12	.78	2.76	4.90	1.62	.17	1.12	98.85	26	232	158
K–2662B	63.68	.82	16.41	5.67	.15	2.02	5.14	4.11	1.34	.26	2.23	97.12	22	317	103
K–2662C	63.87	.83	16.28	5.67	.16	2.03	5.04	4.02	1.43	.26	2.52	96.68	22	317	108
K–2663A	63.79	.81	16.27	5.59	.16	2.01	5.12	4.35	1.23	.26	.35	99.14	22	322	107
K–2663B	63.66	.83	16.67	5.82	.16	2.03	4.94	3.93	1.34	.24	2.93	96.22	26	313	110
Southwest Trident (1953–74)															
K–70	61.64	0.68	16.74	5.81	0.11	2.81	6.47	3.85	1.35	0.14	<0.01	99.37	26	299	138
K–179	59.21	.75	17.00	6.68	.13	3.58	7.27	3.63	1.20	.14	<.01	99.58	23	343	116
K–812	61.61	.63	17.22	5.53	.11	2.61	6.44	3.95	1.35	.15	<.01	100.06	20	309	136
K–1226	59.28	.73	17.15	6.58	.13	3.51	7.25	3.59	1.22	.14	<.01	99.29	27	323	120
K–2027	56.94	.78	17.31	7.42	.14	4.31	8.12	3.39	1.02	.17	–.01	99.37	17	332	99
K–2053	64.77	.68	15.75	5.25	.12	2.12	4.91	4.15	1.69	.17	.01	99.49	33	252	163
K–2146	64.21	.66	16.01	5.24	.12	2.24	5.19	4.13	1.64	.16	.26	99.15	30	269	153
K–2147	63.77	.68	16.01	5.51	.12	2.39	5.31	4.03	1.61	.17	–.03	99.35	30	261	156
K–2148	63.46	.70	15.96	5.69	.12	2.53	5.40	4.00	1.57	.16	–.01	99.25	29	257	152
K–2149	62.58	.72	16.14	5.89	.12	2.74	5.78	3.92	1.51	.21	–.01	99.28	25	265	143
K–2159	61.50	.72	16.35	6.17	.13	3.10	6.20	3.80	1.42	.20	–.06	99.25	26	294	132
K–2172	61.47	.73	16.43	6.14	.13	3.00	6.28	3.82	1.42	.19	–.08	99.48	25	300	133
K–2173	61.40	.72	16.39	6.19	.13	3.20	6.31	3.69	1.40	.17	.02	98.90	27	292	136
K–2174	60.26	.75	16.56	6.53	.13	3.44	6.71	3.70	1.32	.20	–.10	99.75	24	302	127
K–2175	61.12	.73	16.66	6.19	.13	3.08	6.48	3.66	1.37	.17	–.04	98.99	26	301	133
K–2176	58.28	.77	17.01	7.03	.14	4.01	7.55	3.45	1.14	.23	–.14	99.37	21	350	108
K–2177	65.02	.66	15.79	5.16	.11	2.07	4.87	4.05	1.70	.16	.00	99.18	34	271	163
K–2178	61.90	.72	16.32	6.02	.13	2.97	6.07	3.82	1.46	.20	–.04	99.39	31	288	137

clasts in both the pumiceous (unit tig; sample K–2489) and dense-clast (unit tpf; 12 samples, table 2) pyroclastic-flow deposits at Mageik Creek include material more evolved (66.5–71.8 weight percent SiO_2) than any eruptive unit identified elsewhere in the whole Trident group. Moreover, for both units, most samples plot below the main data arrays of the Trident group in the K_2O and Zr panels (figs. 16*A*, 16*C*), suggesting that the magmas which produced the pyroclastic flows either fractionated zircon and a K-bearing phase (neither of which has been recognized elsewhere in the Trident group) or mixed with extraneous rhyolitic melt relatively deficient in K_2O and Zr.

Because these late Pleistocene pyroclastic-flow units are so anomalous compositionally, we infer that their vents have been buried by younger deposits or, alternatively, that any equivalent proximal material was stripped, buried, or never deposited. Potential vents include Trident I, West Trident, and any of the peripheral lava domes (fig. 3).

Warm Springs

Thermal springs south of Trident Volcano were mentioned by Spurr (1900) but not well located on his sketch map. The National Geographic Society expeditions that explored the Katmai Pass area in 1916–19 noted them as well, and their fine topographic map (Griggs, 1922), which was triangulated in the field, located the springs between Mageik Creek and dome 2600+, just east of the main present-day cluster of warm springs (fig. 3). During our own fieldwork in that area (1976–2001), the cluster has been limited to several shallow arroyos cut into 1912 pyroclastic deposits (fig. 17) just beneath the termini of the 1953 and 1958 lava flows from Southwest Trident. Bicarbonate-sulfate waters emerge from dozens of orifices at individual discharge rates of about 5 to 30 L/min (Keith and others, 1992). Most orifice temperatures (measured in July or August of various years, 1976–92) are only 9–28°C, but Keith and others (1992) measured a few at 40–42°C in 1982–84, and Johnston (1979) recorded one spring as hot as 50°C in 1978. About 2 km downstream, several springs of much greater discharge issue from the bedrock walls of Mageik Creek just south of dome 2460 (fig. 3); these measured only 15–20°C in the summers of 1997–98 but were fringed by extensive reddish-orange Fe-rich precipitates.

Another cluster of thermal springs lies 2.5 km south of Katmai Pass, at Ferruginous Flat (fig. 3), where lateral lobes of the 1958 lava flow blocked Mageik Creek, impounding a shallow lake that soon filled with alluvium and became a mudflat. Bicarbonate-sulfate waters discharge at numerous small Fe-precipitating springs that issue at about 15°C from

Figure 17. Warm spring discharging from rhyolitic pumice-fall deposit (not exposed) beneath 1912 ignimbrite, with snout of 1958 andesitic lava flow from Southwest Trident in background (figs. 1, 3). About 10 m of buff nonwelded ignimbrite is separated by 1-m-thick section of 1912 dacite pumice fall from conformably overlying lava flow, which here is 25 to 30 m thick. About 20 such warm springs, typically 25–42°C in summer, discharge near andesite flow fronts and drain along similarly vegetated gullies to Mageik Creek. View northwestward.

the alluvium and along gullies cut in 1912 pyroclastic deposits adjacent to the steep margin of the 1958 lava flow. Total discharge for the whole cluster was estimated by Keith and others (1992) at 100 to 300 L/min in the summers of 1982 and 1984.

On the basis of chemical and isotopic data, Keith and others (1992) reasoned that both sets of spring waters are products of shallow mixing between near-surface waters and a vapor-brine aureole beneath Southwest Trident. The Ferruginous Flat cluster may be influenced by the young cone and its shallow conduit, whereas the southern cluster must tap a deeper-circulating, longer-lived hydrothermal system, possibly heated by the pre-1953 dacitic magma reservoir, which Coombs and others (2000) reckoned to lie at only 3-km depth. Both sets of spring waters contain about 1 ppm As.

Fumaroles

Fumaroles at Trident Volcano likewise form two groups: those on the new composite cone of Southwest Trident and a long-lived fumarole field on the southeast flank of Trident I (fig. 3). The second group contains dozens of fumaroles distributed across a 300-m-wide patch of acid-altered ground that extends about 600 m upslope from 3,600-ft (1,100 m) to as high as 4,500-ft (1,370 m) elevation. First noted in 1916 by Griggs (1922, p. 98–99), in some places the cluster coalesces into a single conspicuous plume, and it always produces a strong odor of H_2S, which can be troublesome for those of us foolish enough to have camped downwind. In 1994–97, Bob Symonds of the USGS Cascades Volcano Observatory took several gas samples here and measured numerous near-boiling temperatures as high as 94°C. Analysis showed that the steam-dominated gas contains abundant CO_2, SO_2, H_2S, H_2, CH_4, and NH_3. Symonds' samples yielded He-isotopic ratios 7.5 times the atmospheric ratio, characteristic of magmatic gas at arc volcanoes, and $\delta^{13}C$ values of CO_2 close to −10 permil, which probably indicate a mixture of magmatic CO_2 and CO_2 derived by thermal breakdown of sedimentary rocks below the volcano.

At the site of Southwest Trident, the first evidence of a fumarole is provided by the set of aerial photographs taken by the Navy in August 1951, in which a conspicuous white plume is seen rising from a 100-m-wide pit on the southwest ridge of Trident I, at precisely the site of the magmatic outbreak that began in February 1953. Because no fumarole had previously been reported at this site, which lay in full view of the trail through Katmai Pass crossed by many parties between the 1890s and the 1930s (Spurr, 1900; Beach, 1909; Griggs, 1922; Hubbard, 1932, 1935), it can be inferred that the fumarolic vent developed during the decade or two before 1951. We are aware of no observational record for the 1940s.

During the main eruptive interval (1953–63), many fumaroles at Southwest Trident were, of course, strongly superheated, but no data are known to have been recorded. When the cone was climbed in August 1963 (by Pete Ward and Bob Decker, then of Dartmouth College), the crater interior was obscured by thick fumarolic cloud, and hundreds of fumarolic orifices lined with molten and crystalline sulfur dotted the entire crater rim (Decker, 1963); most orifices measured were hotter than 200°C, the upper limit of their thermometer. In 1978–79, we observed hundreds of fumaroles still active on and outside the crater rim (especially on the east and south slopes; fig. 14), but all measured were at or below the boiling temperature, 97°C (Johnston, 1979; Sheppard and others, 1992). Some of Johnston's 1978–79 gas samples were analyzed, showing them to be steam dominated but to contain significant concentrations of CO_2 and sulfur (Sheppard and others, 1992). In July 1990, from a fine perspective on the upper slope of Trident I less than 1 km from the steaming cone (but able to see only its east half), we counted 20 fumaroles on a lava bench low on the south flank of the cone, only 10 on lower slopes of the fragmental cone, and at least 100 high on the cone (as in fig. 14). During the 1990s, Bob Symonds measured fumarole temperatures only near or below boiling, the maximum value he recorded declining from 97°C in 1993 to 95°C in 1997. Although hundreds of orifices remain active, the odor of H_2S has abated, from strong in 1979 to barely perceptible in 1997. The H_2S output of Southwest Trident is now insignificant in comparison with that of the fumarole field southeast of Trident I.

Present-Day Seismicity and Deformation

Gravity and seismic data that identify a low-density, low-velocity region centered near Katmai Pass were summarized by Ward and others (1991). A southeasterly gravity traverse that crossed the volcanic axis by way of Katmai Pass showed the cross-axial width of the anomalous region to be about 15 km, but the data are insufficient to know how far it extends along the axis. Of the several seismic stations in Ward's 1987–91 array, only the one in Katmai Pass (central to the gravity anomaly) consistently showed traveltime delays for deep local and regional earthquakes. The delays require great thickness for the low-velocity domain, which may well extend below 20-km depth (Ward and others, 1991), thus involving most or all of the crust. Although their seismic data also indicated significant attenuation of *P* and *S* waves, they observed no screening of *S* waves (in contrast to interpretations of seismic reconnaissance studies 25 years earlier). To explain the data, they invoked present-day crustal magma storage, favoring scattered small magma bodies rather than a large chamber. One such body, of course, erupted to build the Southwest Trident volcano only a few decades ago.

The high rate of shallow microseismicity recognized by Ward and others (1991) has persisted. The Alaska Volcano Observatory expanded the Katmai seismometer network to 18 stations during the 1990s and continues to locate 40 to130 earthquakes each month along and near the volcanic axis (Jolly and McNutt, 1999; Power and others, 2001). Most of the earthquakes fall into three persistent clusters: (1) beneath Martin and Mageik Volcanoes, (2) beneath Katmai Pass and

the northwest slope of the Trident group, and (3) beneath the northwest half of Mount Katmai. Nearly all the earthquakes are of $M<2.5$; most are shallower than 5 km, and nearly all are shallower than 10 km. Such dense shallow microseismicity seems inconsistent with present-day upper-crustal storage of voluminous magma bodies and more likely reflects fluid flow, volume changes, and hydraulic microfracturing in the hydrothermal systems beneath the long-steaming volcanoes, along with slip-threshold reduction in the hydrothermally altered rocks. Nonetheless, in such an environment, dikes and sills or modest pods of magma are by no means excluded, as even a 0.7-km^3-volume pod like that erupted in 1953–74 would be hard to detect by routine seismic methods.

By comparing satellite images taken in 1993 and 1995, Lu and others (1997) used synthetic-aperture-radar interferometry to detect at least 7 cm of uplift beneath Southwest Trident. They interpreted the apparent ground deformation to reflect inflation of a pressure source at only 0.8- to 2-km depth, which they attributed to either magma intrusion or pressurization of the hydrothermal system. Considering the drastic decline in temperature and sulfur output of Southwest Trident fumaroles during the past 25 years, and in light of the field of warm springs conspicuous in the area since at least 1898, a hydrothermal explanation of the various geophysical anomalies is certainly plausible.

Behavior of Glaciers

Trident received a thicker blanket of 1912 fallout from adjacent Novarupta than did any of the other glacier-supporting volcanoes in the Katmai cluster. Moreover, the Knife Creek Glaciers north of Trident were also covered by thin pyroclastic-flow deposits, which ran up the ice and feathered out in the saddles between summits (Fierstein and Hildreth, 1992). We previously described the post-1951 behavior of the shrinking glaciers on nearby Mount Mageik (Hildreth and others, 2000) and the inconsistent patterns of retreat, advance, or stagnation for the several glaciers on Snowy Mountain (Hildreth and others, 2001) and Mount Griggs (Hildreth and others, 2002). Inspection of aerial photographs taken in 1951 and 1987 (respectively, the earliest and most recent sets available) indicates inconsistent behavior for the glaciers on Trident as well. We have observed no measurable changes in terminal positions since 1987, although small ones could have escaped detection.

Glacier 1, westernmost of the Knife Creek Glaciers, is fed largely from cirques below the north face of Trident I and the northwest face of East Trident (figs. 2, 3). Within and below each cirque, the most proximal 800 m or so of the steep and heavily crevassed ice surface has been largely cleared of 1912 pyroclastic deposits, by a combination of outflow and new ice formation. Medial and distal parts of the 4-km-long glacier are still covered, however, by as much as 12 m of 1912 material and locally by more recent avalanche deposits. The glacier terminus, which is steep and active, advanced 250 m between 1951 and 1987, edging out on top of welded 1912 ignimbrite on the floor of uppermost Knife Creek.

Contiguous to the east, Glacier 2 is fed from cirques below the north face and northeast ridge of East Trident. Only 3 km long, it terminates alongside neighboring Glacier 1 at 2,450-ft (750 m) elevation on the floor of Knife Creek (figs. 2, 3). Like its neighbor, only its steep proximal surfaces have been cleared of the thick cover of 1912 pyroclastic debris, of which most (but not all) has been disrupted by ice movement. The glacier terminus advanced more than 300 m between 1951 and 1987, and like its neighbors Glacier 1 and Glacier 3 (which is fed from Mount Katmai), it has overrun the margin of the 1912 ignimbrite.

A pair of small cirque glaciers below the north face of the arête connecting Trident I and West Trident are confluent into an icefall that joins Glacier 1 (fig. 3). Comparison of 1951 and 1987 photographs reveals little change except advanced removal of 1912 fallout from the ice surface.

A small steep slope glacier just below the summit of West Trident, on its northwest face, is only 350 m long but conspicuously crevassed. Although the glacier's margins appear to have changed little, the ice may have thickened substantially between 1951 and 1987. Adjoining snow slopes that cover much of the northwest side of West Trident (fig. 2) have accumulated atop the 1912 fallout, and by surviving summer ablation in most years, they have transformed into substantial fields of névé.

Another small cirque-floor glacier, formerly fed by avalanching of snow from the steep southwest face of Trident I, was 700 m long and still largely mantled by 1912 fallout when it was completely buried by the Southwest Trident cone and 1957 lava flow.

South of the Trident group, the west fork of Wishbone Glacier extends 7 km from the Trident-Katmai saddle to the gorge of Mageik Creek (fig. 3). From the saddle at 4,500 ft (1,370 m) to the terminus at 1,300 ft (400 m), virtually the entire glacier remains blanketed by 1912 fallout. Although the steep debris-covered terminus receded no more than 30 m between 1951 and 1987, the distal 2 km, which is canyon confined, appears to have thinned by about 10 m. Moreover, during that 36-year interval, a supraglacial stream cut an ice-confined channel, 10 to 20 m deep, down the axis of the lower 2 km of the glacier, suggesting virtual stagnation. About 3 km above the terminus, a 1-km-long lateral lobe branches off onto a plateau to the west (fig. 3). Although its pumice-mantled surface has hardly changed, the moderately sloping terminus of the lobe actually advanced about 110 m between 1951 and 1987.

Finally, a south-trending glacier flooring the narrow valley between Trident I and the south ridge of East Trident has wasted drastically. Already largely stagnant in 1951 and melting away beneath the thick blanket of 1912 pumice, the then-2-km-long glacier has since split into two segments, each 600 m long, separated by an 800-m-long gap now occupied by till, reworked pumice, and windows of andesitic lava (fig. 3). The upper segment is a crevassed slope glacier, its surface free of pumice, that drapes steeply down from the summit saddle

of East Trident. The distal segment is a wasting tongue of dead ice wholly buried by the ablation-disturbed pumice.

Acknowledgments

The purple passage quoted as our introductory epigraph typifies the overwrought mythology long attached to Katmai Pass, the only easy route around the Trident group. It recalls memorable days when we cached our packs and fled, but there were also brilliant placid nights when we slept there under the stars, enjoying the gentle seismicity and the airy whiff of brimstone. For cheerful comradeship and strong backs, we thank our Katmai Pass companions down the years, Larry Jager, Dave Johnston, Anita Grunder, Terry Keith, Mike Thompson, and Michelle Coombs. We are grateful to James Saburomaru and Forrest McFarland for K-Ar dating, and to Joel Robinson, who digitally prepared our Katmai geologic map, of which figure 3 is a localized adaptation. Most of the fieldwork was done on foot, but latter-day additions were accomplished with the help of helicopter pilots Paul Walters and Bill Springer. For encouraging completion of this study, we are particularly grateful to Terry Keith, who successively led the Alaska Volcano Observatory and the USGS Volcano Hazards Team.

References Cited

Bacon, C.R., and Druitt, T.H., 1988, Compositional evolution of the zoned calcalkaline magma chamber of Mount Mazama, Crater Lake, Oregon: Contributions to Mineralogy and Petrology, v. 98, no. 2, p. 224–256.

Baedecker, P.A., ed., 1987, Methods for geochemical analysis: U.S. Geological Survey Bulletin 1770.

Beach, Rex, 1909, The Silver Horde; a novel: New York, Harper & Brothers, 390 p. [Relates a crossing of Katmai Pass before the 1912 eruption modified the landscape].

Coombs, M.L., Eichelberger, J.C., and Rutherford, M.J., 2000, Magma storage and mixing conditions for the 1953–1974 eruptions of Southwest Trident volcano, Katmai National Park, Alaska: Contributions to Mineralogy and Petrology, v. 140, no. 1, p. 99–118.

Decker, R.W., 1963, Proposed volcano observatory at Katmai National Monument; a preliminary study: Hanover, N.H., Dartmouth College, report submitted to U.S. National Park Service, 54 p.

Detterman, R.L., Case, J.E., Miller, J.W., Wilson, F.H., and Yount, M.E., 1996, Stratigraphic framework of the Alaska Peninsula: U.S. Geological Survey Bulletin 1969–A, 74 p.

Fierstein, Judy, and Hildreth, Wes, 1992, The plinian eruptions of 1912 at Novarupta, Katmai National Park, Alaska: Bulletin of Volcanology, v. 54, no. 8, p. 646–684.

Fierstein, Judy, and Hildreth, Wes, 2000, Preliminary volcano-hazard assessment for Katmai Volcanic Cluster, Alaska: U.S. Geological Survey Open-File Report 00–489, 50 p.

Gill, J.B., 1981, Orogenic andesites and plate tectonics: Berlin, Springer-Verlag, 390 p.

Griggs, R.F., 1922, The Valley of Ten Thousand Smokes: Washington, D.C., National Geographic Society, 340 p.

Hildreth, Wes, 1983, The compositionally zoned eruption of 1912 in the Valley of Ten Thousand Smokes, Katmai National Park, Alaska: Journal of Volcanology and Geothermal Research, v. 18, no. 1–4, p. 1–56.

———1987, New perspectives on the eruption of 1912 in the Valley of Ten Thousand Smokes, Katmai National Park, Alaska: Bulletin of Volcanology, v. 49, no. 5, p. 680–693.

———1990, Trident, Alaska Peninsula, in Wood, C.A., and Kienle, Jürgen, eds., Volcanoes of North America; United States and Canada: New York, Cambridge University Press, p. 68–69.

———1991, The timing of caldera collapse at Mount Katmai in response to magma withdrawal toward Novarupta: Geophysical Research Letters, v. 18, no. 8, p. 1541–1544.

Hildreth, Wes, and Fierstein, Judy, 2000, Katmai volcanic cluster and the great eruption of 1912: Geological Society of America Bulletin, v. 112, no. 10, p. 1594–1620.

———2003, Geologic map of the Katmai volcanic cluster, Katmai National Park, Alaska: U.S. Geological Survey Miscellaneous Investigations Series Map I–2778, scale 1: 63,360.

Hildreth, Wes, Fierstein, Judy, Lanphere, M.A., and Siems, D.F., 1999, Alagogshak volcano; a Pleistocene andesite-dacite stratovolcano in Katmai National Park, *in* Kelley, K.D., ed., Geologic studies in Alaska by the U.S. Geological Survey, 1997: U.S. Geological Survey Professional Paper 1614, p. 105–113.

———2000, Mount Mageik: A compound stratovolcano in Katmai National Park, *in* Kelley, K.D., and Gough, L.P., eds., Geologic studies in Alaska by the U.S. Geological Survey, 1998: U.S. Geological Survey Professional Paper 1615, p. 23–41.

———2001, Snowy Mountain; a pair of small andesite-dacite stratovolcanoes in Katmai National Park, *in* Gough, L.P., and Wilson, F.H., eds., Geologic studies in Alaska by the U.S. Geological Survey, 1999: U.S. Geological Survey Professional Paper 1633, p. 13–34.

———2002, Mount Griggs: A compositionally distinctive Quaternary stratovolcano behind the main volcanic line in Katmai National Park, *in* Wilson, F.H., and Galloway, J.P., eds., Geologic Studies in Alaska by the U.S. Geological Survey, 2000: U.S. Geological Survey Professional Paper 1662, p. 87–112.

Hildreth, Wes, and Lanphere, M.A., 1994, Potassium-argon geochronology of a basalt-andesite-dacite arc system; the Mount Adams volcanic field, Cascade Range of southern Washington: Geological Society of America Bulletin, v. 106, no. 11, p. 1413–1429.

Hildreth, Wes, Lanphere, M.A., and Fierstein, Judy, 2003, Geochronology and eruptive history of the Katmai volcanic cluster, Alaska Peninsula: Earth and Planetary Science Letters, v. 214, p. 93–114.

Hubbard, B.R., 1932, Mush, you malemutes!: New York, America Press, 179 p.

———1935, Cradle of the storms: New York, Dodd, Mead & Co., 285 p.

Johnston, D.A., 1979, Volcanic gas studies at Alaskan volcanoes, *in* Johnson, K.M., and Williams, J.R., eds., The United States Geological Survey in Alaska; accomplishments during 1978: U.S. Geological Survey Circular 804–B, p. B83–B84.

Jolly, A.D., and McNutt, S.R., 1999, Seismicity at the volcanoes of Katmai National Park, Alaska; July 1995–December 1997: Journal of Volcanology and Geothermal Research, v. 93, no. 3–4, p. 173–190.

Keith, T.E.C., Thompson, J.N., Hutchinson, R.A., and White, L.D., 1992, Geochemistry of waters in the Valley of Ten Thousand Smokes region, Alaska: Journal of Volcanology and Geothermal Research, v. 49, no. 3–4, p. 209–231.

Kienle, Jürgen, Swanson, S.E., and Pulpan, Hans, 1983, Magmatism and subduction in the eastern Aleutian arc, *in* Shimozuru, Daisuke, and Yokoyama, Izumi, eds., Arc volcanism—physics and tectonics: Tokyo, Terra Scientific, p. 191–224.

Kosco, D.G., 1981, Characteristics of andesitic to dacitic volcanism at Katmai National Park, Alaska: Berkeley, University of California, Ph.D. thesis, 249 p.

Lanphere, M.A., 2000, Comparison of conventional K-Ar and $^{40}Ar/^{39}Ar$ dating of young mafic volcanic rocks: Quaternary Research, v. 53, no. 3, p. 294–301.

Lu, Zhong, Fatland, D.R., Wyss, Max, Eichelberger, J.C., Dean, Kenneson, and Freymueller, J.T., 1997, Deformation of New Trident volcano measured by ERS–1 SAR interferometry, Katmai National Park, Alaska: Geophysical Research Letters, v. 24, no. 6, p. 695–698.

Miyashiro, Akiho, 1974, Volcanic rock series in island arcs and active continental margins: American Journal of Science, v. 274, no. 4, p. 321–355.

Muller, E.H., Juhle, R.W., and Coulter, H.W., 1954, Current volcanic activity in Katmai National Monument: Science, v. 119, no. 3088, p. 319–321.

Peacock, M.A., 1931, Classification of igneous rock series: Journal of Geology, v. 39, no. 1, p. 54–67.

Plafker, George, Moore, J.C., and Winkler, G.R., 1994, Geology of the southern Alaska margin, chapter 12 *of* Plafker, George, and Berg, H.C., eds., The geology of Alaska, v. G–1 of The geology of North America: Boulder, Colo., Geological Society of America, p. 389–449.

Power, J.A., Moran, S.C., McNutt, S.R., Stihler, S.D., and Sanchez, J.J., 2001, Seismic response of the Katmai volcanoes to the 6 December 1999 magnitude 7.0 Karluk Lake earthquake, Alaska: Seismological Society of America Bulletin, v. 91, no. 1, p. 57–63.

Ray, D.K., 1967, Geochemistry and petrology of the Mt. Trident andesites, Katmai National Monument, Alaska: Fairbanks, University of Alaska, Ph.D. thesis, 198 p.

Riehle, J.R., Detterman, R.L., Yount, M.E., and Miller, J.W., 1993, Geologic map of the Mount Katmai quadrangle and adjacent parts of the Naknek and Afognak quadrangles, Alaska: U.S. Geological Survey Miscellaneous Investigations Series Map I–2204, scale 1:250,000.

Sheppard, D.S., Janik, C.J., and Keith, T.E.C., 1992, A comparison of gas geochemistry of fumaroles in the 1912 ash-flow sheet and on active stratovolcanoes, Katmai National Park, Alaska: Journal of Volcanology and Geothermal Research, v. 53, no. 1–4, p. 185–197.

Simkin, Tom, and Siebert, Lee, 1994, Volcanoes of the world; a regional directory, gazetteer, and chronology of volcanism during the last 10,000 years (2d ed.): Tucson, Geoscience Press, 349 p.

Snyder, G.L., 1954, Eruption of Trident volcano, Katmai National Monument, Alaska: U.S. Geological Survey Circular 318, 7 p.

Spurr, J.E., 1900, A reconnaissance in southwestern Alaska in 1898, *in* Explorations in Alaska in 1898: U.S. Geological Survey Annual Report 1898–1899, pt. 7, p. 31–264.

Stacey, J.S., Sherrill, N.D., Dalrymple, G.B., Lanphere, M.A., and Carpenter, N.V., 1981, A five-collector system for the simultaneous measurement of argon isotope ratios in a static mass spectrometer: International Journal of Mass Spectrometry & Ion Physics, v. 39, p. 167–180.

Ward, P.L., and Matumoto, Tosimatu, 1967, A summary of volcanic and seismic activity in Katmai National Monument, Alaska: Bulletin Volcanologique, v. 31, p. 107–129.

Ward, P.L., Pitt, A.M., and Endo, Elliot, 1991, Seismic evidence for magma in the vicinity of Mt. Katmai, Alaska: Geophysical Research Letters, v. 18, no. 8, p. 1537–1540.

Wilson, F.H., 1985, The Meshik arc—an Eocene to earliest Miocene magmatic arc on the Alaska Peninsula: Alaska Division of Geological and Geophysical Surveys Professional Report 88, 14 p.